

# Influence of parameterization changes on Arctic low cloud properties and cloud radiative effects in two versions of the HadGEM3 Atmospheric Model: GA7.1 and GA6

Patrick Charles Taylor<sup>1</sup>, Robyn C. Boeke<sup>2</sup>, and Alejandro Bodas-Salcedo<sup>3</sup>

<sup>1</sup>National Aeronautics and Space Administration (NASA)

<sup>2</sup>Science Systems and Applications, Inc.

<sup>3</sup>Met Office Hadley Centre

March 04, 2024

## Abstract

Arctic clouds play a key role in Arctic climate variability and change; however, contemporary climate models struggle to simulate cloud properties accurately. Model-simulated cloud properties are determined by the physical parameterizations and their interactions within the model configuration. Quantifying effects of individual parameterization changes on model-simulated clouds informs efforts to improve cloud properties in models and provides insights on climate system behavior. This study quantifies the influence of individual parameterization schemes on Arctic low cloud properties within the Hadley Centre Global Environmental Model 3 atmospheric model using a suite of experiments where individual parameterization packages are changed one-at-a-time between two configurations: GA6 and GA7.1. The results indicate that individual parameterization changes explain most of the cloud property differences, whereas multiple parameterizations, including non-cloud schemes, contribute to cloud radiative effect differences. The influence of a parameterization change on cloud properties is found to vary by meteorological regime. We employ a three-term decomposition to quantify contributions from (1) regime independent, (2) regime dependent, and (3) the regime frequency of occurrence changes. Decomposition results indicate that each term contributes differently to each cloud property change and that non-cloud parameterization changes make a substantial contribution to the LW and SW cloud radiative effects by modifying clear-sky fluxes differently across regimes. The analysis provides insights on the role of non-cloud parameterizations for setting cloud radiative effects, a model pathway for cloud-atmosphere circulation interactions, and raises questions on the most useful observational approaches for improving models.

# **Influence of parameterization changes on Arctic low cloud properties and cloud radiative effects in two versions of the HadGEM3 Atmospheric Model: GA7.1 and GA6**

Patrick C. Taylor<sup>1,\*</sup>, Robyn C. Boeke<sup>2</sup>, Alejandro Bodas-Salcedo<sup>3</sup>

<sup>1</sup>NASA Langley Research Center, Hampton, VA, USA

<sup>2</sup>Analytical Mechanical Associates, Hampton, VA, USA

<sup>3</sup>Met Office Hadley Centre, Exeter, UK

## Key Messages:

- Individual parameterization changes explain cloud property changes and multiple parameterizations explain cloud radiative effect changes.
- The large-scale cloud scheme is the single most impactful parameterization to changes in Arctic meteorological regime frequency.
- Non-cloud parameterizations must be considered to understand the full influence of parameterization changes on cloud radiative effects.

\*Corresponding author email: [patrick.c.taylor@nasa.gov](mailto:patrick.c.taylor@nasa.gov)

## Abstract

Arctic clouds play a key role in Arctic climate variability and change; however, contemporary climate models struggle to simulate cloud properties accurately. Model-simulated cloud properties are determined by the physical parameterizations and their interactions within the model configuration. Quantifying effects of individual parameterization changes on model-simulated clouds informs efforts to improve cloud properties in models and provides insights on climate system behavior. This study quantifies the influence of individual parameterization schemes on Arctic low cloud properties within the Hadley Centre Global Environmental Model 3 atmospheric model using a suite of experiments where individual parameterization packages are changed one-at-a-time between two configurations: GA6 and GA7.1. The results indicate that individual parameterization changes explain most of the cloud property differences, whereas multiple parameterizations, including non-cloud schemes, contribute to cloud radiative effect differences. The influence of a parameterization change on cloud properties is found to vary by meteorological regime. We employ a three-term decomposition to quantify contributions from (1) regime independent, (2) regime dependent, and (3) the regime frequency of occurrence changes. Decomposition results indicate that each term contributes differently to each cloud property change and that non-cloud parameterization changes make a substantial contribution to the LW and SW cloud radiative effects by modifying clear-sky fluxes differently across regimes. The analysis provides insights on the role of non-cloud parameterizations for setting cloud radiative effects, a model pathway for cloud-atmosphere circulation interactions, and raises questions on the most useful observational approaches for improving models.

## **Plain Language Summary**

Arctic clouds play a key role in Arctic climate variability and change; however, state-of-the-art climate models struggle to simulate cloud properties accurately. Errors in model-simulated cloud have known and unknown influences on the simulated climate state and climate change projections. Model cloud properties are determined by the physical parameterizations and their interactions within the model. Thus, to improve model-simulated clouds, we need to understand the effects of parameterization changes. We use a series of Hadley Centre Global Environmental Model 3 atmospheric model simulations where individual parameterizations are changed one-at-a-time. This approach allows us to isolate the influence of individual cloud parameterizations on model-simulated cloud properties to inform model development and the observations needed to improve models. The results show that individual parameterizations are most important for specific cloud variables and that multiple parameterizations are important to determining the model-simulated influence of clouds on the energy budget. We also find that changes in model-simulated cloud properties respond differently under different weather conditions. The analysis provides insights on the role of non-cloud parameterizations for setting cloud radiative effects, the ways that clouds and the atmosphere interact, and raises questions on the most useful observational approaches for improving models.

## 1. Introduction

The Arctic is rapidly changing; observed and simulated surface temperature trends are larger than any other region (e.g., Taylor et al. 2017; Chylek et al. 2021; Rantanen et al. 2022). Climate change simulations point to an acceleration of Arctic warming through the 21<sup>st</sup> century; however, the climate model projected warming rate has a large inter-model spread (e.g., Previdi et al. 2021; Taylor et al. 2022). Narrowing the spread in future predictions is a key scientific challenge requiring improved knowledge of the processes driving Arctic change.

Cloud feedbacks are an important factor in global and Arctic climate change (Zelinka et al. 2020; Ceppi et al. 2021; Hahn et al. 2021; Tan et al. 2023; McGraw et al. 2023). A change in Arctic cloud properties in response to surface warming can affect the Arctic climate system by modulating the thermodynamic structure of the Arctic atmosphere, altering the surface energy budget, masking the radiative response of sea ice loss, and changing the mass balance of Arctic sea ice (Curry et al. 1996; Vihma et al. 2014; Tan et al. 2019; Sledd and L'Ecuyer 2019; Alkama et al. 2020; Sledd and L'Ecuyer 2021). The magnitude of Arctic cloud feedback varies substantially across contemporary climate models and impacts the projection of Arctic warming and sea ice loss (e.g., Boeke and Taylor 2018; Hahn et al. 2021; Tan et al. 2019). Thus, a better representation of Arctic cloud properties and evolution within climate models will help narrow the spread in Arctic cloud feedback and climate change projections.

Recent studies highlight model-observational discrepancies in Arctic cloud properties and indicate that model-simulated cloud biases stem from multiple sources. In Coupled Model Intercomparison Project 5 (CMIP5) models, Boeke and Taylor (2016) show that model-simulated clouds are too reflective in summer and not insulating enough in winter. These errors in the cloud radiative effects are related to too little cloud amount, too little cloud liquid, too much cloud ice,

and errors in the seasonal evolution of cloud properties (e.g., Komurcu et al. 2014; Klaus et al. 2016; Taylor and Boeke 2016; Taylor et al. 2019). These model-observational differences in CMIP5 models generally remain in CMIP6 (e.g., Tselioudis et al. 2021). Cloud microphysical and aerosol parameterizations strongly affect model-simulated cloud properties and radiative effects but are not the only contributing factors (e.g., Gettelman et al. 2010; Komurcu et al. 2014; English et al. 2014; Taylor et al. 2015; Klaus et al. 2016; Morrison et al. 2018; Taylor et al. 2019; Tan and Barahona 2022; Tan et al. 2023). Pithan et al. (2014) explore ‘clear’ and ‘cloudy’ states of the Arctic wintertime boundary layer finding that the transition between mixed phase and ice clouds is not only a function of cloud microphysics, but also a result of a change in meteorological regimes and dynamical interactions. This suggests that the frequency of meteorological regimes can also substantially influence model-simulated cloud properties (e.g., Stramler et al. 2011; Morrison et al. 2012). These results underscore the importance of understanding the influence of specific parameterizations on simulated cloud properties and the dependence on meteorological regime.

This study aims to advance our understanding of the multiple influences on model-simulated Arctic low cloud properties. The experimental approach employed uses simulations from two consecutive configurations of the atmospheric component of the Hadley Centre Global Environmental Model (HadGEM) GA6 and GA7.1. This study leverages HadGEM3 cloud parameterization experiments from Bodas-Salcedo et al. (2019) that individually turn on/off parameterization package updates between GA6 and GA7.1 to assess the influence of each on simulated Arctic cloud properties. The study stratifies cloud properties and radiative effects by meteorological regimes, following Taylor et al. (2019), to investigate the dependence of the cloud property response to parameterization changes on meteorological conditions. The results are compared to Clouds and the Earth’s Radiant Energy System (CERES) observations and the

Modern-Era Retrospective analysis for Research and Applications-2 (MERRA-2). The study objective is to determine the most important parameterizations affecting Arctic cloud properties in HadGEM3 and evaluate the alignment with observations.

## **2. Model, Data, and Methodology**

### 2.1. Model Description

The analysis uses the two configurations of the HadGEM3 atmosphere model—GA6 and GA7.1. These configurations are set apart by the suite of parameterization updates from GA6 to GA7.1. To make the number of simulations manageable, individual updates are grouped into development “packages”, as in Bodas-Salcedo et al. (2019). A package is a collection of parameterization changes that are related, either because they modify the same physical parameterization (e.g., convection) or because they are logically dependent. A complete list of model changes introduced between GA6 and GA7.1 can be found in Walters et al. (2019) and Mulcahy et al. (2018), and a description of the packages in Bodas-Salcedo et al. (2019). We provide a brief description of the individual package changes that explain most of the differences in the simulation of Arctic clouds between GA7.1 and GA6.

#### 2.1.1. Large-scale cloud

The large-scale cloud scheme is responsible for the calculation of the cloud fraction and condensate within each gridbox at each timestep (Wilson et al. 2008a,b; Morcrette 2012; Van Weverberg et al. 2016). The primary changes in this package are listed below.

- Radiative impact of convective cores: the profiles of convective cloud amount and cloud condensate are combined with the large-scale cloud fields before being passed to the cloud generator of the radiative transfer code.

- Consistent treatment of phase change for convective condensate passed to large-scale cloud: this change enforces consistency between the upper temperature limit at which ice can be formed by convection and in the large-scale cloud scheme.
- Turbulence-based critical relative humidity: the value of the critical relative humidity used to initiate cloud in cloud-free grid boxes or to remove cloud from cloud-filled grid boxes has changed from being constant at each model level to being dependent on sub-grid turbulence.
- Removal of redundant complexity for ice cloud: this removes the effect of two ice cloud fraction increment terms that partially offset and had no clear physical justification.
- A retuning of the low cloud was carried out with the aim of reducing its albedo while maintaining the improved cloud cover.

#### 2.1.2. Radiation

The radiation code updates the vertical profiles of heating rates in each gridbox due to radiative processes in the solar and terrestrial parts of the spectrum (Edwards and Slingo, 1996; Manners et al., 2015). The changes in this package are listed below.

- Consistent ice optical and microphysical properties: update of the parameterization for scalar optical properties of ice crystals to the formulation by Baran et al. (2016).
- Revised ice microphysical properties: the representation of ice particle size distribution is updated to the empirical distribution of Field et al. (2007), and the mass-diameter relation is updated based upon measurements with improved accuracy (Cotton et al. 2013).
- Improved treatment of gaseous absorption: improved representation of H<sub>2</sub>O, CO<sub>2</sub>, O<sub>3</sub> and O<sub>2</sub> absorption in the SW and of all gases in the LW.

#### 2.1.3. Microphysics

This package bundles changes related to large-scale precipitation or strongly coupled to microphysical processes, as listed below.

- Improved treatment of sub-grid-scale cloud water content variability: parameterization of the fractional standard deviation of cloud water content as formulated in Hill et al. (2015).
- New warm rain microphysics: re-write of the warm rain part of the large-scale precipitation scheme, as documented in Boutle and Abel (2012) and Boutle et al. (2014).
- Turbulent production of liquid water in mixed-phase cloud: implementation of a new parameterization of liquid water production in mixed-phase cloud (Field et al. 2014; Furtado et al. 2016).

## 2.2. Model Experiments

The model experiment suite consists of a series of 14-year AMIP-style simulations where the updated development packages are turned on/off individually to target either GA7.1 (using GA6 as a baseline and turning an updated package on) or GA6 (using GA7.1 as a baseline and turning an updated package off). The union of all packages contain all changes between GA6 and GA7.1.

Daily and monthly data are used from March 2000 to December 2014. Due to the large number of parameterization package changes between GA6 and GA7.1, monthly output is used to identify the packages with the greatest effect on monthly mean cloud properties (not shown). Table 1 lists the ten individual parameterizations and two combinations that have the largest impact on monthly mean cloud properties. The analysis described in Section 3 uses daily output from GA6\_ON

experiments; simulations using the base GA6 model where a single parameterization scheme is updated to the GA7.1 parameterization one at a time, hereafter called ON\_experiments.

**Table 1.** Summary of the development packages analyzed.

<b>Name</b>	<b>Parameterization Package</b>
Rad	Radiation
Aer	Aerosols
Mic	Microphysics and large-scale precipitation
Cld	Large-scale cloud
Cnv	Convection
BL	Boundary layer
GWD	Gravity wave drag
Dyn	Dynamics
Sto	Stochastic physics
Lnd	Land surface
AerErf	Aerosols + Effective radiative forcing
MicCldRad	Microphysics and large-scale precipitation + Large-scale cloud + Radiation

### 2.3. Data and Reanalysis

#### 2.3.1. Clouds and Earth’s Radiant Energy System (CERES)

The CERES synoptic edition 4A product (SYN Ed4a, Doelling et al. 2013; 2016) provides 1-hourly radiative fluxes at the surface, four atmospheric levels (850, 500, 200, and 70 hPa), and the top of the atmosphere (TOA) at  $1^\circ \times 1^\circ$  spatial resolution. The in-atmosphere and surface fluxes are computed hourly using the Langley-modified Fu–Liou radiative transfer model using inputs from the Moderate Resolution Imaging Spectroradiometer (MODIS) and meteorological state from the Goddard Earth Observing System Version 5.4.1 (GEOS-5.4.1; Rutan et al., 2015). Cloud properties are retrieved within four layers: low (surface to 700 hPa), middle (700–500 hPa), middle-high (500–300 hPa), and high (300–50 hPa). Cloud radiative effect (CRE) is defined as the difference between all-sky minus clear-sky fluxes in the LW and SW using downwelling fluxes only to minimize the impact of surface albedo differences. Radiative flux uncertainty of  $\pm 12 \text{ W m}^{-2}$  is adopted for clear-sky fluxes and  $\pm 16 \text{ W m}^{-2}$  for all-sky fluxes and CRE following Kato et al.

(2010; 2011). These uncertainty estimates align with a recent comparison between CERES SYN Ed4a and surface radiometer measurements during the Multidisciplinary drifting Observatory for the Study of Arctic Climate (Huang et al. 2022).

### 2.3.2. MERRA-2

MERRA-2 (Gelaro et al. 2017) is the latest reanalysis produced by the Goddard Modeling and Assimilation Office (GMAO). MERRA-2 uses version 5.12.4 of the GEOS atmospheric model and data assimilation system with horizontal resolution of  $0.58^\circ$  latitude by  $0.6258^\circ$  longitude with a vertical resolution of 72 hybrid-eta levels at 1-hourly temporal resolution (Molod et al. 2015). For this study, MERRA-2 cloud liquid and ice water concentration (CLW and CLI, respectively) profiles are compared with the GA6 and GA7.1 (GMAO 2015).

### 2.4. Meteorological Regime Framework

The meteorological regime framework enables the quantification of differences between models and observations and between model experiments on a regimes-by-regime basis. Meteorological regime analysis provides insights into the processes that influence cloud properties

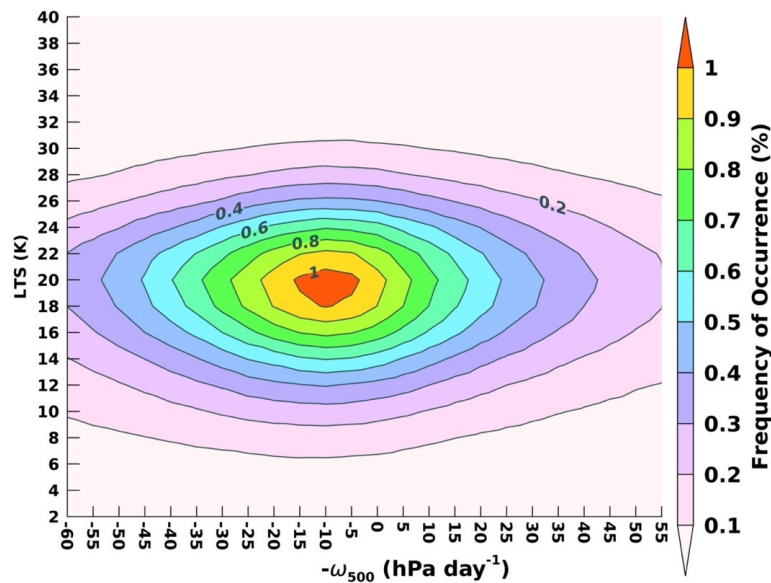


**Figure 1:** Relative frequency of occurrence (RFO) for the meteorological regime phase space of (x-axis) 500 hPa vertical velocity ( $\omega_{500}$ ) and (y-axis) lower tropospheric stability (LTS) for GA6.  $-\omega_{500}$  is used to have ascending motion be represented as a positive number.

under specific atmospheric conditions (e.g., Stramler et al. 2011; Barton et al. 2012; Liu and Schweiger 2017; Taylor et al. 2015; 2019; Zelinka et al. 2023). Studies show that Arctic low cloud amount (LCA) and CLI and CLW are strongly influenced by lower tropospheric stability (LTS) and 500 hPa vertical velocity ( $\omega_{500}$ ) (Solomon et al. 2011; 2014; Shupe et al. 2013; Taylor et al. 2019; Yu et al. 2019; Taylor and Monroe 2023); thus, we stratify cloud properties by these variables to determine regime dependent differences. Figure 1 shows the relative frequency of occurrence (hereafter RFO) of GA6 LTS/ $-\omega_{500}$  meteorological regimes. The most frequent regimes show mid-high stability (LTS  $\sim$  19 K) and weak subsidence ( $-\omega_{500} \sim -10$  hPa day $^{-1}$ ; vertical velocity is expressed  $-\omega_{500}$  for ease of interpretation, positive values indicate rising motion).

Using the RFO and the LCA in each LTS/ $-\omega_{500}$  bin, the average cloud amount can be defined as

$$\overline{LCA} = \sum_{i,j} LCA(LTS_i, -\omega_{500,j}) \cdot RFO(LTS_i, -\omega_{500,j}) \quad (1)$$

where  $LCA(LTS_i, -\omega_{500,j})$  is the average low cloud amount and  $RFO(LTS_i, -\omega_{500,j})$  is the relative frequency of occurrence of the  $i^{\text{th}}$  and  $j^{\text{th}}$  LTS/ $-\omega_{500,j}$  bin. The summation of RFO over all  $i,j$  bins equals one. Applying a first-order Taylor series approximation of (1) and reordering terms allows for the separation of the GA7.1 minus GA6 differences ( $\delta\overline{LCA}_{GA7.1-GA6}$ ) into three terms,

$$\delta\overline{LCA}_{GA7.1-GA6} = \sum_{i,j} \delta LCA'(LTS_i, -\omega_{500,j})_{GA7.1-GA6} \cdot RFO(LTS_i, -\omega_{500,j})_{GA6} + \delta\overline{LCA}_{GA7.1-GA6, equal} \cdot RFO(LTS_i, -\omega_{500,j})_{GA6} + LCA(LTS_i, -\omega_{500,j})_{GA6} \cdot \delta RFO(LTS_i, -\omega_{500,j})_{GA7.1-GA6} \quad (2)$$

where  $\delta\overline{LCA}$  (left-hand side of (2)) is the total difference in LCA between GA7.1 minus GA6. The three terms on the righthand side of (2) from top to bottom represent (a) regime independent, (b) regime dependent, and (c) RFO contributions to total cloud property changes. The regime

independent and dependent terms are determined by defining  $\delta LCA(LTS_i, -\omega_{500,j})_{GA7.1-GA6}$  as the sum of  $\delta \overline{LCA}_{GA7.1-GA6, equal} + \delta LCA'(LTS_i, -\omega_{500,j})_{GA7.1-GA6}$ .

$$\delta \overline{LCA}_{GA7.1-GA6, equal} = \frac{1}{N} \sum_{i,j} \delta LCA(LTS_i, -\omega_{500,j})_{GA7.1-GA6} \quad \text{and} \quad (3)$$

$$\begin{aligned} \delta LCA'(LTS_i, -\omega_{500,j})_{GA7.1-GA6} \\ = \delta LCA(LTS_i, -\omega_{500,j}) - \delta \overline{LCA}_{GA7.1-GA6, equal} \end{aligned} \quad (4).$$

The regime independent term,  $\delta \overline{LCA}_{GA7.1-GA6, equal}$ , represents the equal-weight average cloud property change across all  $LTS_i/-\omega_{500,j}$  bins, where  $N$  is the total number of bins. The regime dependent term,  $\delta LCA'(LTS_i, -\omega_{500,j})_{GA7.1-GA6}$ , represents the deviation of the cloud properties within a regime from the equal-weight averaged GA7.1-GA6 difference across all regimes. The RFO term represents the contributions to the GA7.1-GA6 differences from shifts in regime frequency. Equation (2) is applied to LCA, CLI, CLW, and LW and SW CRE to quantify the relative contributions of these terms to inter-model and model-observation differences.

### 3. Results

#### 3.1. GA7.1 and GA6 differences

This section documents the cloud properties and radiative flux changes between GA6 and GA7.1. To provide a comprehensive perspective of these differences, we present a comparison of the Arctic domain average and meteorological regime average cloud properties.

Table 2 summarizes the Arctic domain average cloud properties and LW and SW CRE for GA6 and differences with GA7.1 and the ON\_experiments (discussed in Section 3b). The final line in Table 2 shows the linear combination of the individual ON\_experiments and AerErf\_ON; MicCldRad\_ON and Aer\_ON are not included in this sum to avoid double counting. This line can be compared to the full difference GA7.1 - GA6 (Table 2, line 2) indicating a greater degree of

closure for cloud property variables than for radiative fluxes. A comparison with observations is provided in Section 3c. Table 2 indicates that GA7.1 has less LCA than GA6 in the annual mean and in each season (not shown). Conversely, GA7.1 shows greater annual mean and seasonal CLI and CLW in the lower atmosphere than GA6.

**Table 2.** Summary of Arctic domain average cloud properties and radiative effects for model simulations, where RLSDSCS, RSDSCS, and RSUSCS represent the downwelling longwave clear-sky flux, the downwelling shortwave clear-sky flux, and the upwelling shortwave clear-sky flux at the surface.

	<i>CA</i> (%)	<i>CLI</i> (g kg <sup>-1</sup> )	<i>CLW</i> (g kg <sup>-1</sup> )	<i>LWCRE</i> (W m <sup>-2</sup> )	<i>RLSDSCS</i> (W m <sup>-2</sup> )	<i>SWCRE</i> (W m <sup>-2</sup> )	<i>RSDSCS</i> (W m <sup>-2</sup> )	<i>RSUSCS</i> (W m <sup>-2</sup> )
<b>GA6</b>	29.70	5.96	5.67	39.66	204.27	-44.71	146.32	58.32
<b>GA7.1-GA6</b>	-6.02	3.33	2.32	2.78	1.14	-0.01	-3.51	-3.95
<i>Rad_ON-GA6</i>	0.72	2.49	0.02	1.17	1.47	0.81	-1.75	-0.99
<i>Aer_ON-GA6</i>	0.30	0.14	-0.11	1.52	-1.95	-1.69	-0.58	-0.08
<i>Mic_ON-GA6</i>	1.07	0.22	1.30	1.05	-1.31	-2.47	0.10	0.18
<i>Cld_ON-GA6</i>	-8.80	-0.63	0.07	-4.17	-2.42	5.66	0.25	0.72
<i>Cnv_ON-GA6</i>	0.61	0.33	-0.18	0.70	-1.47	-1.14	0.24	0.10
<i>BL_ON-GA6</i>	0.23	0.56	-0.04	0.69	0.06	-1.26	0.03	-0.10
<i>GWD_ON-GA6</i>	-0.59	-0.10	-0.18	-0.95	0.13	1.13	-0.04	-0.23
<i>Dyn_ON-GA6</i>	-0.46	-0.07	-0.01	-0.32	-0.34	0.20	-0.06	-0.22
<i>Sto_ON-GA6</i>	-0.08	0.11	-0.02	0.66	0.08	-1.06	-0.06	-0.11
<i>Lnd_ON-GA6</i>	-0.52	-0.02	0.21	0.25	2.98	-0.30	-0.59	-2.75
<i>AerErf_ON-GA6</i>	0.17	0.18	0.03	1.27	-0.63	-0.40	-1.46	-2.41
<i>MicCldRad_ON-GA6</i>	-6.54	1.78	1.26	-1.60	-1.42	4.00	-1.37	0.10
<b>Sum of ON_Experiments</b>	-7.67	3.07	1.19	0.35	-1.43	1.17	-3.35	-5.81
<b>CERES</b>	40.7	--	--	43.8	209.0	-43.1	141.6	46.1
<b>MERRA-2</b>	--	1.12	20.9	--	--	--	--	--

The domain average cloud property changes compete in their influence on LW and SW CRE.

The result shows that GA7.1 has a larger annual mean LW CRE than GA6 and in each season except for June-July-August (not shown). SW CRE shows little change in the annual mean due to offsetting seasonal differences: GA7.1 more negative than GA6 in spring and less negative in summer. GA7.1 has a greater downwelling clear-sky LW flux and less downwelling and upwelling clear-sky SW flux at the surface. The clear-sky flux changes impact the CREs, where the increased

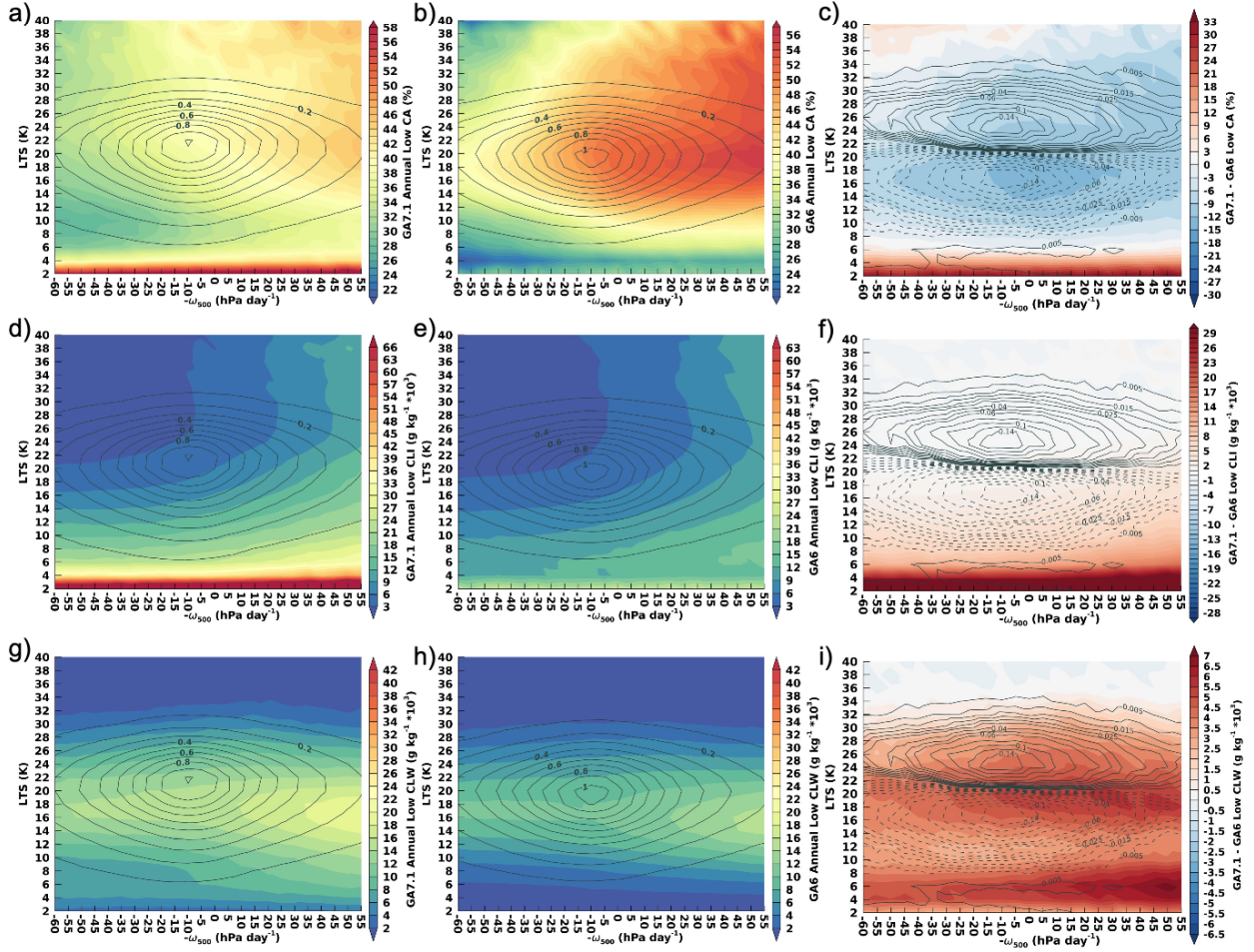


**Figure 2.** Annual mean (a-c) low cloud amount, (d-f) cloud ice mixing ratio (units:  $\text{g kg}^{-1}$ ), and (g-i) cloud liquid mixing ratio (units:  $\text{g kg}^{-1}$ ) within LTS/ $-\omega_{500}$  meteorological regimes for GA7.1, GA6, and GA7.1-GA6 differences, respectively.

downwelling LW clear-sky flux reduces GA7.1 minus GA6 LW CRE difference. In the SW, the reductions in downwelling SW clear-sky fluxes offset the influence of increased CLW and CLI. Overall, Table 2 illustrates substantial changes in domain average cloud properties, CRE, and clear-sky fluxes between GA7.1 and GA6.

We find that domain average changes are not distributed evenly across meteorological regimes. Figure 2 shows the average LCA, CLI, and CLW values within the LTS/ $-\omega_{500}$  regimes for GA7.1, GA6, and the GA7.1 minus GA6 differences. For LCA, the smaller GA7.1 average LCA results from a general reduction in LCA across a range of the most frequently occurring regimes (Fig. 2c); the largest LCA reductions are found in regimes with LTS between 12-20 K and weak to moderate

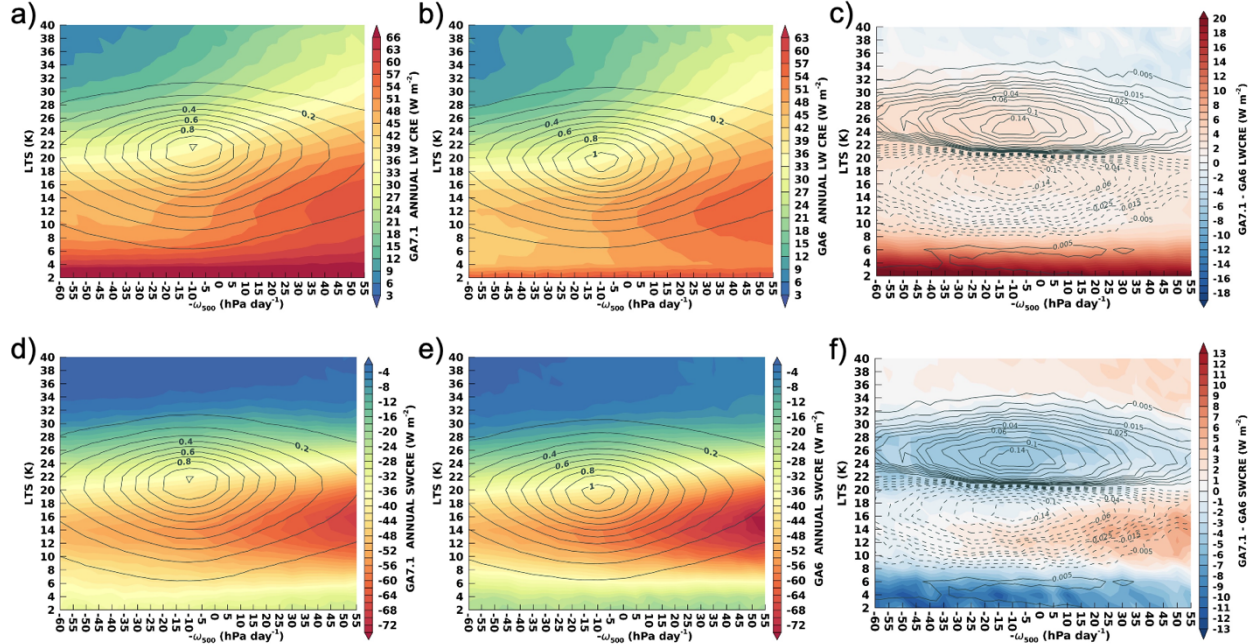


**Figure 3.** Annual mean (a-c) LW CRE and (d-f) SW CRE within LTS/ $\omega_{500}$  meteorological regimes for GA7.1, GA6, and GA7.1-GA6 differences. Units are  $\text{W m}^{-2}$ .

rising motion. Large increases in LCA (exceeding 20%) are found at  $\text{LTS} < 4 \text{ K}$ . However, these LCA increases do not contribute substantially to the domain average due to their low RFO.

Meteorological regime dependent differences between GA7.1 and GA6 are also found for CLI and CLW. The greater domain average CLI in GA7.1 (Fig. 2f) is supported by small increases across many meteorological regimes with the largest increases at  $\text{LTS} < 12 \text{ K}$  (Fig. 2f); these increases show a weak dependence on  $\omega_{500}$ . In contrast, CLW differences between GA7.1 and GA6 vary with  $\omega_{500}$  and the strongest CLW increases occur in regimes of rising motion. The larger domain average GA7.1 CLW is supported by strong increases across a range of LTS values from 2-32 K (Fig. 2i). The meteorological regimes that show the largest increases in CLW also show the largest reductions in LCA. Large increases in CLI and CLW are also found at  $\text{LTS} < 4 \text{ K}$ .

The distribution of LW and SW CRE changes between GA7.1 and GA6 across meteorological regimes result from the competing influences of LCA and CLW changes (Fig. 3). GA7.1 shows greater LW CRE than GA6 across most meteorological regimes with a few meteorological regimes

showing greater increases, including at  $LTS < 8$  K and under moderate subsidence conditions with LTS between 20-28K. For SW CRE, the GA7.1-GA6 differences vary strongly across meteorological regimes; more negative differences are found at  $LTS < 6$  K and between 22-30 K. GA7.1 shows more positive SW CRE than GA6 at LTS between 10-16 K. The results indicate that for regimes where LW CRE increases and SW CRE decreases the CLW increase dominates the CRE change, whereas in the regimes where LW CRE decreases and SW CRE increases the LCA decrease dominates.

Changes in meteorological regime RFO also influence the GA7.1-GA6 differences. The solid and dotted contours in Fig. 2c indicates a RFO shift toward increased LTS in GA7.1 than GA6. This shift reduces the impact of LCA reductions as the regimes with the greatest reductions also have reduced RFOs. Conversely, the CLW increase and the increased LW and SW CRE magnitudes in GA7.1 contribute more strongly to the domain average, as regimes with increased RFO show a greater CLW increase. The RFO changes play a minor role in CLI differences. Clear from Fig. 2 and 3, the domain averaged differences in the cloud properties are influenced by a combination of changes in meteorological regime cloud properties and changes in regime RFO. To quantify the influence of RFO, we apply the decomposition in (2)-(4).

Different terms of the decomposition (Fig. 4) dominate the GA7.1-GA6 differences for different cloud variables. The regime independent term accounts for the largest contribution to the CLI, CLW, and LW CRE differences. For CLI, the regime dependent term partly offsets the regime independent term. The regime dependent term makes the largest contribution to the LCA reduction from GA6 to GA7.1. The RFO term makes the largest contribution to the SW CRE differences.

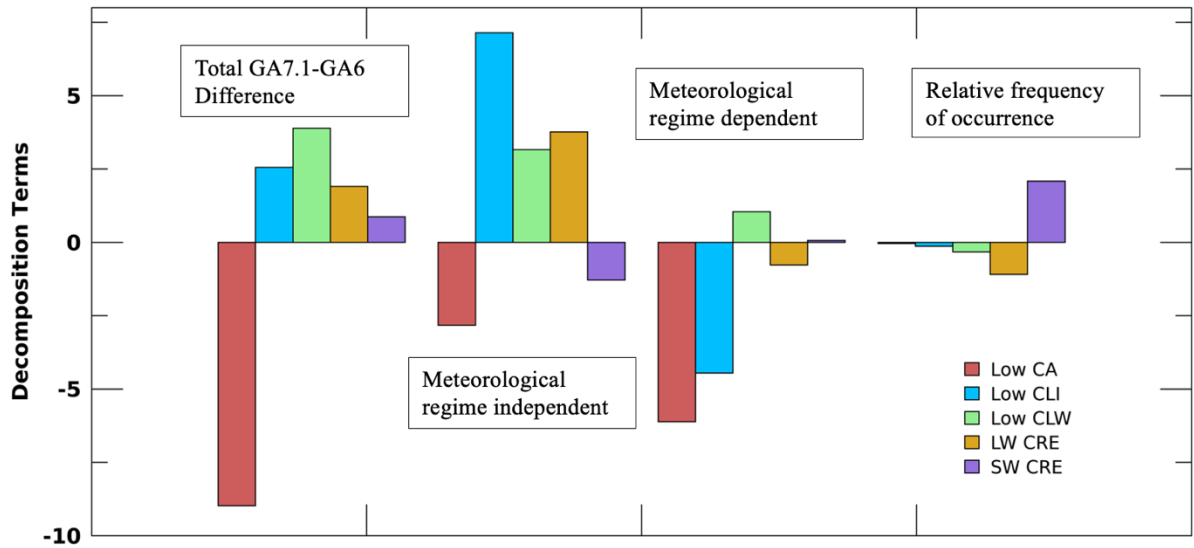


**Figure 4.** Annual mean contributions (units: %, g kg<sup>-1</sup>, and Wm<sup>-2</sup>) from left to right are the total GA7.1-GA6 difference, meteorological regime independent, meteorological regime dependent, and relative frequency of occurrence contributions to (red) LCA, (blue) CLI, (green) CLW, (gold) LW CRE, and (purple) SW CRE.

The results indicate that when assessing the factors that influence the changes in the cloud and radiative properties one cannot assume that the factors that determine the change in one cloud property also explain the change in another.

### 3.2. Role of individual parameterizations

Many parameterization updates make up the evolution from GA6 to GA7; however, the results show that a handful explain most of the cloud property differences. Using the suite of ON\_experiments (Table 1), we quantify the influence of individual parameterization schemes on the GA7.1 minus GA6 cloud differences. Two of the ON\_experiments are combinations of parameterization scheme changes: AerErf\_ON and MicCldRad\_ON.

The analysis of domain average cloud property and CRE changes for the ON\_experiments indicate that the parameterization packages that most strongly influence the GA7.1-GA6 differences are different for each cloud variable. For cloud properties, the annual mean domain average change from GA6 to GA7.1 (Table 2) is explained by a single package change: Cld\_ON for LCA, Rad\_ON for CLI, and Mic\_ON for CLW. For LCA and CLW, most ON\_experiments

do not produce a substantial domain average change. For CLI, several ON\_experiments alter the GA6 domain average by more than  $\sim 10\%$ , including Cld\_ON and BL\_ON. These effects are, however, substantially less than the  $\sim 40\%$  change in Rad\_ON. Considering LCA, Cld\_ON overshoots the GA7.1 domain average but considering multiple package changes simultaneously (MicCldRad\_ON) the agreement with GA7.1 LCA is within  $\sim 0.5\%$ .

In contrast to cloud properties, multiple package changes are needed to explain the LW and SW CRE GA7.1-GA6 differences. The LW CRE differences between GA7.1 and GA6 (Table 2) is  $\sim 7\%$ . Most ON\_experiments do not produce a large change. Aer\_ON produces the greatest increase in LW CRE and most closely matches GA7.1 but is only 55% of the total GA7.1-GA6 difference. The largest absolute change is a decrease in LW CRE found in Cld\_ON, due to the reductions in LCA. Considering SW CRE, the overall GA7.1-GA6 difference is small resulting

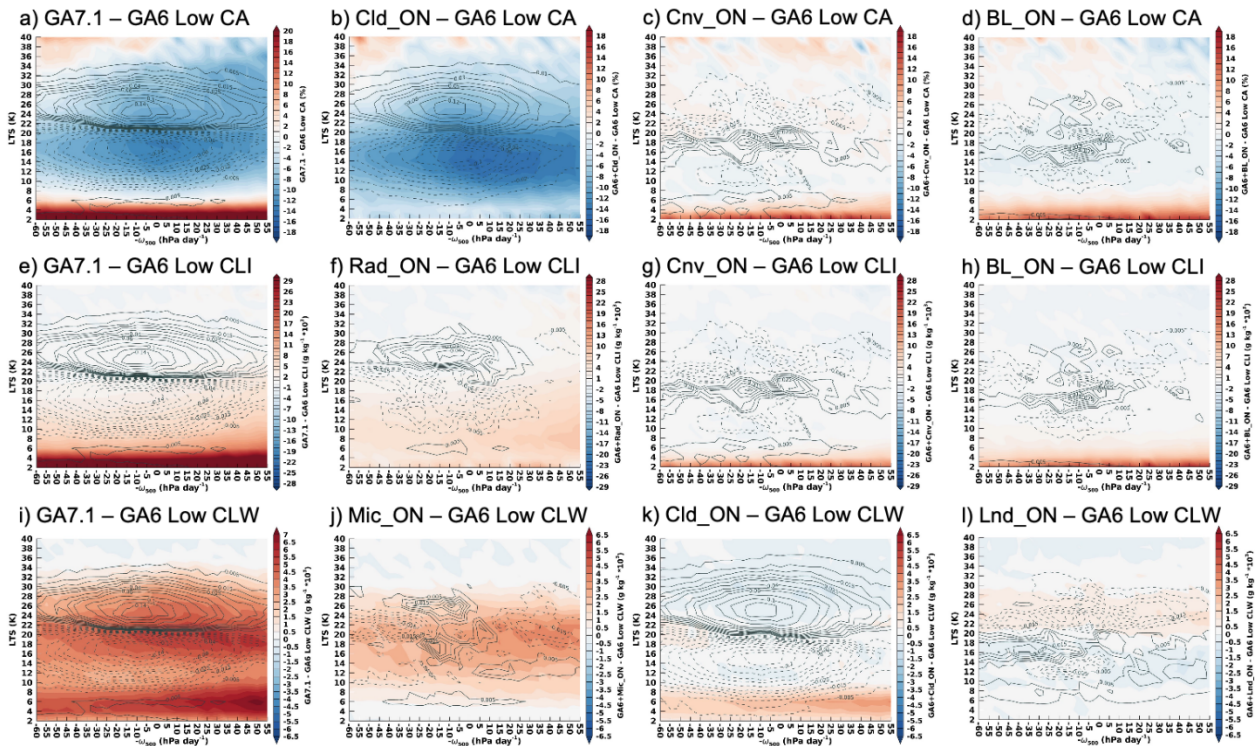


**Figure 5:** Annual mean differences between GA7.1 and GA6 and ON\_experiments and GA6 for (a-d) LCA, (e-h) CLI, and (i-l) CLW. Panels (a, e, i) GA7.1 minus GA6, (b, k) Cld\_ON minus GA6, (c, g) Cnv\_ON minus GA6, (d, h) BL\_ON minus GA6, (f) Rad\_ON minus GA6, (j) Mic\_ON minus GA6, and (l) Lnd\_ON minus GA6.

from offsetting effects of many parameterization changes.

As opposed to the domain average changes, multiple parameterization package changes are needed to explain the cloud property differences across meteorological regimes. Considering LCA, Fig. 5 shows that the Cld\_ON, Conv\_ON, and BL\_On experiments influence the distribution of GA7.1-GA6 cloud property changes across meteorological regimes. Cld\_ON (Fig. 5b) produces a general LCA decrease across most regimes; the Conv\_ON and BL\_ON experiments (Fig. 5c,d) are responsible for the LCA increase at LTS < 6 K. For CLI, Rad\_ON (Fig. 5f) produces the general CLI increase when LTS < 22 K and, as with LCA, Conv\_ON and BL\_ON experiments (Fig. 5g,h) are responsible for the CLI increase at LTS < 6 K. For CLW, Mic\_ON (Fig. 5j) produces the increase in CLW at LTS values between 10 and 28 K. Different from LCA and CLI, Cld\_ON (Fig. 5k) contains the increased CLW at LTS < 8 K, not Conv\_ON and BL\_ON.

Multiple parameterization packages are also needed to explain the LW and SW CRE changes across meteorological regimes. Interestingly, the MicCldRad\_ON experiment (Fig. 6b,g), which captures cloud property changes well, does not reproduce the LW and SW CRE GA7.1-GA6 differences in the domain average or in meteorological regimes. BL\_ON (Fig. 6c,h), Aer\_ON (Fig.

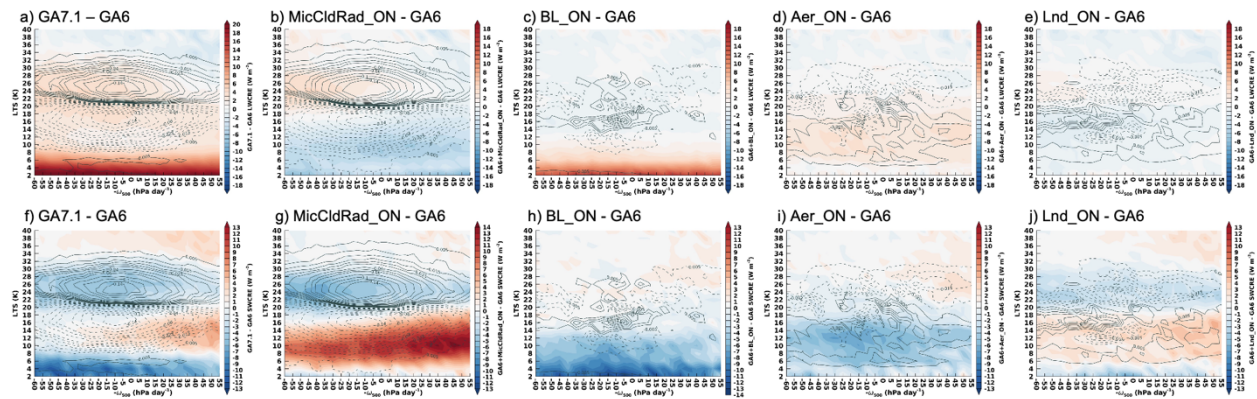


**Figure 6.** Annual mean differences between GA7.1 and GA6 and ON experiments and GA6 for (a-e) LW CRE and (f-j) SW CRE. Panels (a,f) GA7.1-GA6, (b,g) MicCldRad\_ON-GA6, (c,h) BL\_ON-GA6, (d,i) Aer\_ON-GA6, (e,j) Land\_ON-GA6. Units are  $W m^{-2}$ .

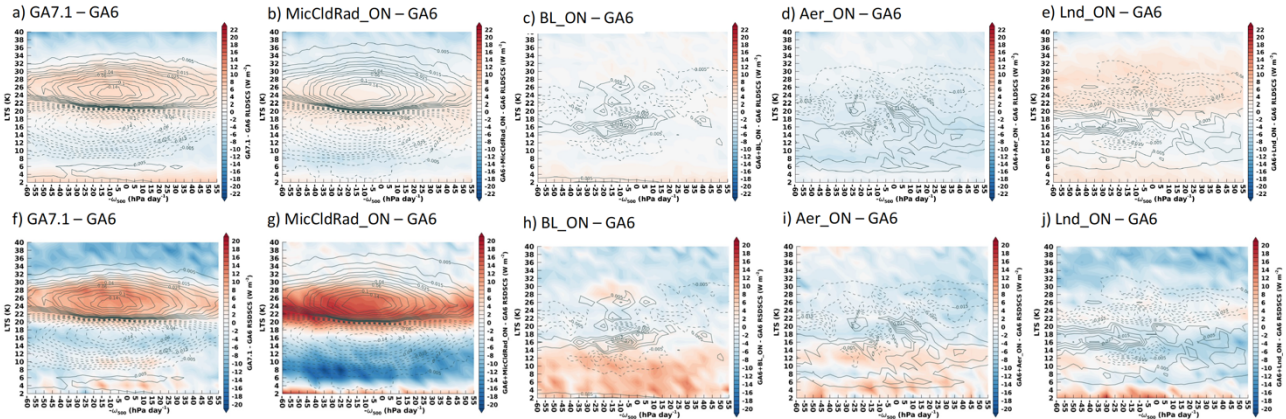


**Figure 7.** Annual mean differences in RLDSCS (a) GA7.1 - GA6, b) MicCldRad\_ON - GA6; c) BL\_ON - GA6; d) Aer\_ON - GA6 and e) Lnd\_ON - GA6. Figures (f) to (j): as (a) to (e) but for RSDSCS. Units are  $Wm^{-2}$ .

6d,i), and Lnd\_On (Fig. 6e,j) experiments also substantially influence the LW and SW CRE changes across meteorological regimes. This indicates that packages that do not influence cloud properties (referred to as “non-cloud” changes) influence the simulated LW and SW CRE.

We find that non-cloud parameterization packages substantially influence the GA7.1-GA6 LW and SW CRE differences by affecting the clear-sky fluxes. Considering RLDSCS, MicCldRad\_ON (Fig. 7b) and Lnd\_ON (Fig. 7e) exhibit a pattern that most closely resembles GA7.1-GA6 (Fig. 7a). In the available simulations, Lnd\_ON produces the largest positive change in RLDSCS. For RSDSCS (Fig. 7f-j), MicCldRad\_ON shows a strong influence on the RSDSCS with a similar pattern to GA7.1-GA6 (Fig. 7f) but stronger with a magnitude. Cloud parameterization changes contribute to substantial increases in RSDSCS for LTS from 20 to 28K and substantial decreases for LTS from 4-16 K. Several non-cloud scheme changes, including BL\_ON (Fig. 7h) and Aer\_On (Fig. 7i), offset these impacts on RSDSCS. The results indicate that the clear-sky flux response to cloud and non-cloud parameterization changes substantially influence LW and SW CRE.

Different ON\_experiments produce different RFO patterns, however Cld\_ON and Rad\_ON dominate the overall GA7.1-GA6 differences. The pattern shown by most ON\_experiments (Fig. 5) is a weak increase in the RFO for LTS from 14 to 22 K and a decrease in RFO at slightly larger

and smaller LTS with a weak  $-\omega_{500}$  dependence. Several parameterizations, specifically Mic\_ON (Fig. 5j) and Sto\_ON (not shown), show a RFO change with a greater dependence on  $-\omega_{500}$ . Most ON\_experiments show small RFO changes with a pattern that does not resemble GA7.1-GA6 differences (Fig. 5). Cld\_ON (Fig. 5b) and Rad\_ON (Fig. 5f) experiments show RFO change patterns that closely correspond to GA7.1-GA6. The RFO changes in the Rad\_ON experiment are  $\sim 25\%$  of the changes found in Cld\_ON. Thus, the Cld\_ON experiment provides the strongest influence on GA7.1-GA6 RFO changes. The results provide no evidence for a strong non-cloud parameterization influence on regime RFO changes.

Figure 8 shows a bar chart where the left most grouping represents the total cloud property change between GA7.1 (black bars) or an ON\_experiment (colored bars) and GA6. The remaining Fig. 8 groupings represent the regime independent, atmospheric regime dependent, and RFO terms, respectively. Considering LCA changes, the Cld\_ON experiment dominates the overall change; however, the regime independent term makes the largest contributions in Cld\_ON,

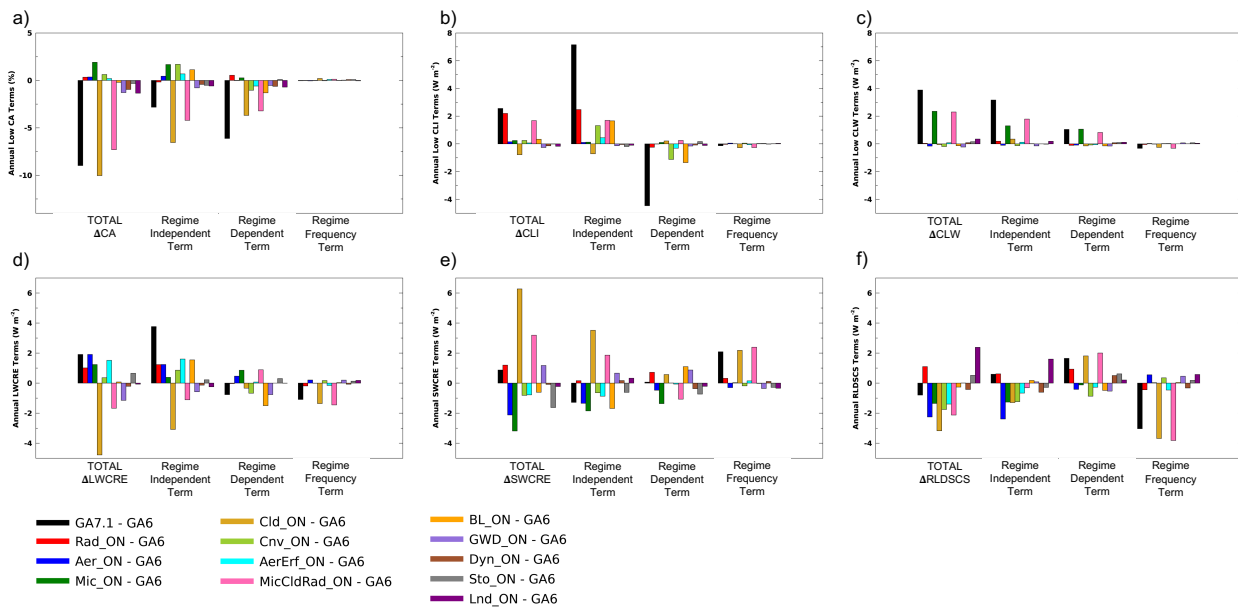


**Figure 8:** Contributions of the atmospheric-regime independent, atmospheric-regime dependent, and frequency of meteorological regime occurrence terms to the (a) LCA, (b) CLI, (c) CLW, (d) LW CRE, (e) SW CRE, and (f) RLDSCS to the annual mean GA7.1-GA6 and ON\_experiment-GA6 differences.

differing from Fig. 4 where the regime dependent term makes the largest contribution. Considering the CLI change, the overall contribution is dominated by Rad\_ON (as in Table 2). Rad\_ON, however, only influences the regime independent term while the GA7.1-GA6 change is from offsetting contributions of the regime independent and dependent terms. For CLW, Mic\_ON dominates the overall change and indicates little contribution from other experiments. The decomposition shows that other packages influence CLI but that their net contributions are small due to offsetting contributions from the regime independent and dependent terms. Since Rad\_ON does not produce a strong regime dependent contribution and the other ON\_experiments exhibit offsetting contributions, the source of the large negative contribution from the regime dependent term is unclear; parameterization interactions may explain this contribution.

For LW and SW CRE, many ON\_experiments contribute to the GA7.1-GA6 differences that provide contributions from all three decomposition terms. The Cld\_ON experiment shows offsetting contributions from the regime independent and RFO terms. This is interesting because the RFO change only has a substantial influence on the radiative flux terms and not the cloud property terms. As eluded to previously, the non-cloud parameterization experiments influence LW CRE by influencing the RLDSCS; Fig. 8 indicates that many parameterizations influence this flux. It is interesting that the primary way that the convection scheme influences LW CRE is through an influence on the RLDSCS flux. Lastly, while not making substantial contributions to the overall GA7.1-GA6 changes in any variable, the BL\_ON experiment shows offsetting contributions from the regime independent and dependent terms.

### 3.3. GA7.1 and GA6 differences from observations and reanalysis

This section compares GA7.1 and GA6 cloud properties with CERES SYN Ed4a and MERRA-2 to assess the alignment with observations. Comparisons are performed using average LCA, CLI,

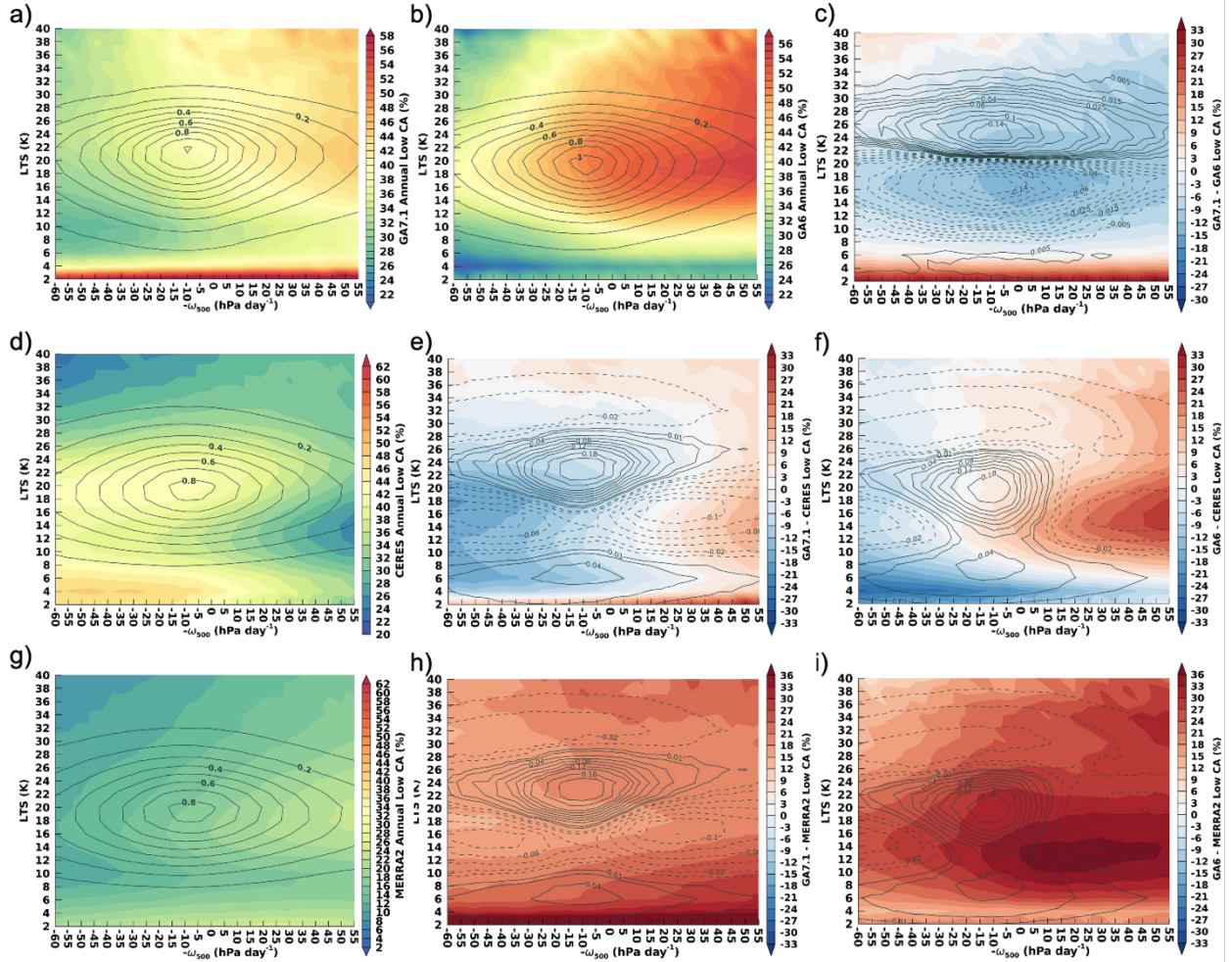


**Figure 9:** Annual mean LCA within LTS/ $-\omega_{500}$  meteorological regimes for (a) GA7.1, (b) GA6, (d) CERES, and (g) MERRA-2 and the (c) GA7.1-GA6, (e) GA7.1-CERES, (f) GA6-CERES, (h) GA7.1-MERRA-2, and (i) GA6-MERRA-2 differences.

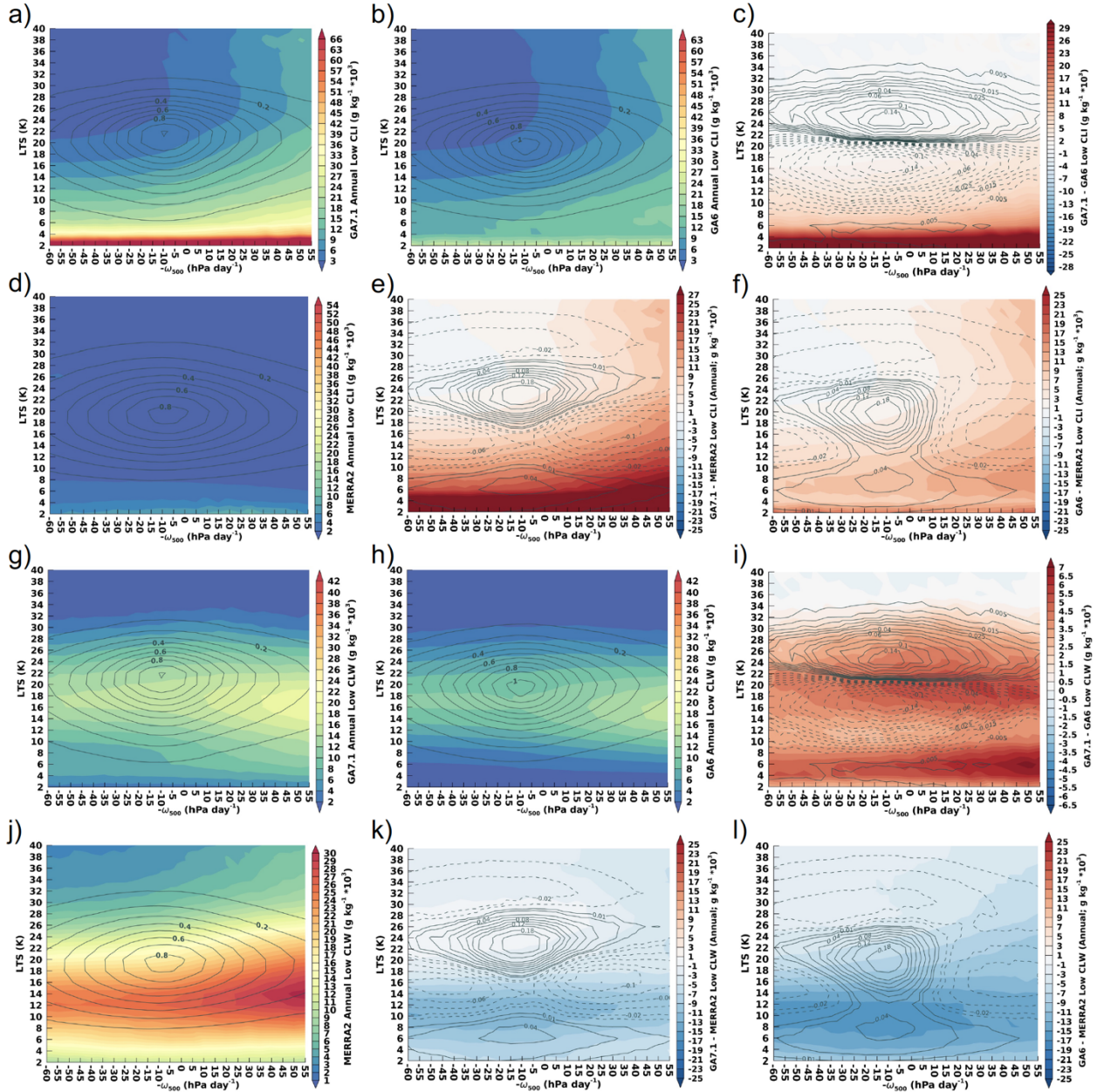
and CLW between the surface and 700 hPa for consistency with the CERES low cloud definition. Computing CRE using only downwelling all- and clear-sky fluxes reduces the impact of surface albedo differences between models and observations.

Figure 9 shows LCA across LTS/ $-\omega_{500}$  regimes for CERES, MERRA-2, and difference plots with GA6 and GA7.1. The LCA joint distributions for GA6, GA7.1 and MERRA-2 indicate increasing LCA for GA regimes with rising motion and medium-high stability (LTS  $\sim$  18 K) while CERES shows more clouds for subsidence regimes. The smaller LCA values for CERES clouds in regimes with rising motion result from passive satellite observations being blind to low clouds

under high clouds. Spaceborne radar measurements show that low clouds are found in these regimes (e.g., Taylor et al. 2015; Yu et al. 2019). Performing this comparison using satellite simulator output is a better method (e.g., Bodas-Salcedo et al. 2011; Kay et al. 2012; Medeiros et al. 2023), however satellite simulator output is not available for these simulations. While MERRA-2 possesses shortcomings in its representation of Arctic low clouds producing too few clouds (Segal Rozenhaimer et al. 2018); the differences between GA7.1 and GA6 with MERRA-2 are the most appropriate comparison for assessing alignment with the observed Arctic clouds. All reanalysis products exhibit shortcomings in the Arctic (Yeo et al. 2022); MERRA-2 is used here as it provides a reasonable representation of the general Arctic cloud properties.

GA6 and GA7.1 LCA compare similarly with MERRA-2 showing the largest differences under rising motion and lower LTS values. The GA7.1 and GA6 also show RFO differences with MERRA-2 (Table 2); however, these differences have a small influence. While GA6 and GA7.1 simulate less LCA than found in MERRA-2, Fig. 9 indicates that GA7.1 is in better overall agreement with MERRA-2.

GA6 and GA7.1 both simulate greater CLI and less CLW than MERRA-2. Figure 10 shows joint distributions for CLI and CLW from reanalysis and differences with GA6 and GA7.1. The greatest CLI for both models and MERRA-2 is found in low stability regimes ( $LTS < 4K$ ), though magnitudes vary greatly. Outside of these low stability regimes, model simulations show a similar dependence of CLI and similar differences with MERRA-2. The GA7.1 and GA6 differences with MERRA-2 are generally regime independent. While the differences between GA7.1 and GA6 with MERRA-2 are substantial, the results suggest that GA6 CLI agrees better with MERRA-2 and GA7.1 shows better agreement with MERRA-2 for CLW.



**Figure 10.** Annual mean (a-f) CLI and (g-l) CLW within LTS/ $-\omega_{500}$  meteorological regimes for (a,g) GA7.1, (b,h) GA6, and (d,j) MERRA-2 and the (c,i) GA7.1-GA6, (e,k) GA7.1-MERRA-2, and (f,l) GA6-MERRA-2 differences. Units are in  $10^{-3} \text{ g kg}^{-1}$

Figure 11 shows the joint distributions of observed and modeled LW CRE (Fig 11a-f) and SW CRE (Fig 11g-l). Maximum LW CRE occurs at  $\sim \text{LTS} < 20 \text{ K}$  for both CERES and models and increases with decreasing stability, though both GA6 and GA7.1 show a dependence on  $-\omega_{500}$  that is not found in observations. CERES LW CRE is larger than GA6 and GA7.1 for mid-high stability

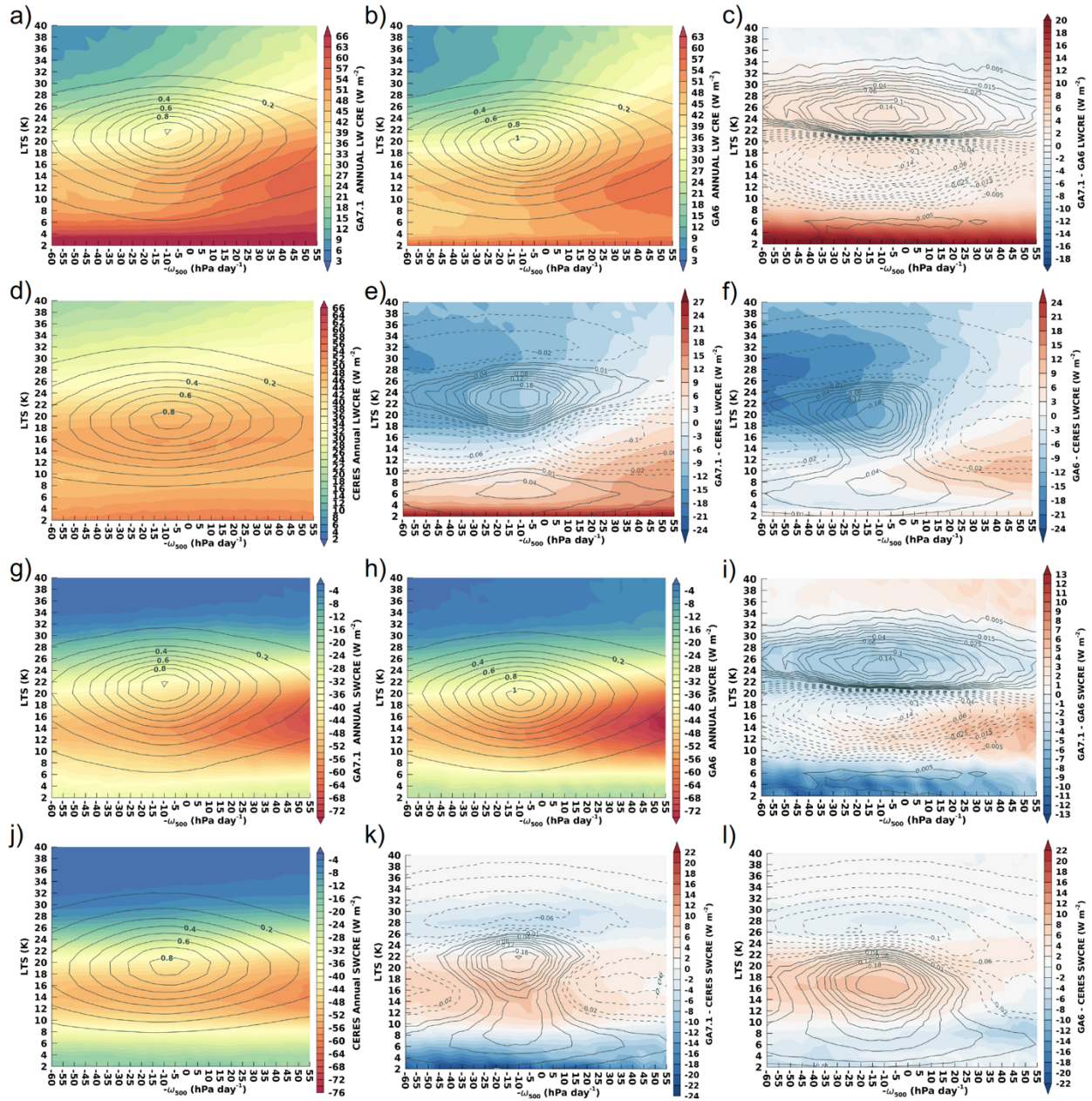


**Figure 11.** Annual mean (a-f) LW and (g-l) SW CRE within LTS/ $-\omega_{500}$  meteorological regimes for (a,g) GA7.1, (b,h) GA6, and (d, j) CERES and the (c, i) GA7.1-GA6, (e,k) GA7.1-CERES, and (f,l) GA6-CERES differences. Units are in  $\text{Wm}^{-2}$ .

regimes, particularly with increasing subsidence. Negative LW CRE differences occur in regimes more frequently simulated by models and contribute to the lower model mean LW CRE. Both GA7.1 and GA6 simulate low stability regimes more frequently than MERRA-2, which for GA7.1 contain mostly positive LW CRE differences ( $\text{GA7.1} > \text{CERES}$ ) while for GA6 these regimes have smaller, slightly negative LW CRE differences ( $\text{CERES} > \text{GA6}$ ). The largest model

differences in LW CRE (Fig. 11c) occur for low stability regimes coinciding with the large inter-model differences in ice clouds present at  $LTS < 4$  K, indicating that changes in CLI are driving radiative differences in GA7.1 farther from CERES observations.

Considering SW CRE (Figure 11g-l), maximum SW CRE for GA6, GA7.1 and CERES is found for rising motion and medium stability with minimum SW CRE found in high stability regimes independent of  $-\omega_{500}$ . These regimes are more frequently simulated in GA7.1 than GA6 (solid line contours in Fig. 11i) and possess larger SW CRE, larger LW CRE, about the same CLI, more CLW, and smaller LCA for GA7.1 compared to GA6. These more frequently simulated regimes do not coincide with the largest inter-model differences and, in the case of LCA, are not coincident with the sign of the largest inter-model differences. If the frequency of low stability regimes increases—either through model improvement or from climate change—larger inter-model biases may be seen.

The takeaway from this comparison is that overall GA7.1 shows better agreement with observations than GA6. However, this is not the case under all conditions. The most notable regimes under which GA6 outperforms GA7.1 are those with low LTS conditions. Overall, GA6 and GA7.1 cloud properties tend to be more like each other than like MERRA-2.

#### 4. Discussion

The conventional approach for improving model-simulated cloud properties and their radiative effects revolves around using (new) in situ or satellite observations to guide the refinement of an existing cloud parameterization or development of a new one (e.g., Field et al. 2007; Molod 2012; Morcrette 2012; Bouttle and Abel 2012; Bouttle et al. 2014; Barahona et al. 2014; Molod et al. 2015). At the heart of this conventional approach is a cloud parameterization. However, a key finding of this paper is the influence of non-cloud parameterizations on LW and SW CRE through

their impact on clear-sky fluxes. The importance of clear-sky fluxes to CRE is evident the definition of CRE and has been discussed in many previous studies (e.g., Sohn et al. 2006; Soden et al. 2008; Boeke and Taylor 2016; Loeb et al. 2020). The influence of cloud parameterization on model-simulated CRE is clear and we document the substantial contributions of non-cloud parameterizations. To the best of our knowledge the contributions of non-cloud parameterizations to model-simulated CRE have not been documented. Thus, non-cloud parameterizations must be considered to understand the full influence of parameterization changes on CRE.

Cloud parameterizations are also found to influence clear-sky fluxes and do so differently by meteorological regime. The influence of cloud parameterizations on clear-sky fluxes indicates a potential feedback/interaction between the cloud properties, the atmospheric circulation, and the clear-sky fluxes that requires further exploration to understand. This effect differs from the influence of different definitions of clear-sky fluxes on CRE.

Many studies highlight the importance of two-way interactions between clouds and the atmospheric circulation (e.g., Li et al. 2015; Ceppi and Hartman 2016; Voigt et al. 2021). We find that the large-scale cloud scheme is the single most impactful parameterization on the changes in the frequency of Arctic meteorological regimes between GA6 and GA7.1. It is known that the large-scale atmospheric circulation responds to the influence of clouds on the atmospheric heating rate profile. Assuming that the cloud influence on the atmospheric heating rate profile is determined to first order by the presence or absence of clouds, it follows that the parameterization that dictates cloud amount would strongly impact the regime RFO. It is not clear, however, why other parameterizations do not more strongly influence the RFO. This result suggests, at least for this model, that cloud presence plays the most important role in determining the meteorological regime occurrence. Thus, this effect could represent an important interaction between clouds and

regime occurrence that enables other mechanisms to influence the atmospheric circulation by impacting cloud amount. For instance, a response of clouds to sea ice loss (e.g., Kay and Gettelman 2009; Taylor et al. 2015; Morrison et al. 2018) could alter the cloud amount and modulate the atmospheric circulation. There has been much debate over the influence of sea ice loss on the Arctic-mid latitude circulation (e.g., Cohen et al. 2020) and Arctic Amplification (Hahn et al. 2021; Taylor et al. 2022; Tan et al. 2023) and this result suggests that a portion of the uncertainty could be related to the cloud response to sea ice.

The present study informs observations in two important ways. First, the RFO distribution indicates the specific atmospheric conditions that make the largest contributions to the mean model-simulated cloud properties and radiative effects. Thus, targeted observation campaigns gathering cloud properties and process data within these most frequently occurring regimes will provide the most value for improving the mean model-simulated cloud properties.

Secondly, the analysis identifies atmospheric conditions with the largest differences between the models and observations; regimes of the greatest differences should also be targeted. Weak LTS regimes and strong LTS regimes under subsidence show the largest difference. This provokes an interesting notion and question. Could cloud properties within infrequently occurring regimes have a strong influence on the atmospheric circulation and the model-simulated response to climate change? Weak LTS regimes and strong LTS regimes under subsidence occur infrequently and, thus, do not significantly contribute to the domain-averaged differences between the models or with observations. Is there value in chasing observations of these infrequently occurring regimes? It is an open question as to whether the most frequently occurring regimes, the regimes with the largest sensitivity, or other regimes are most important to the climate change simulations.

It is clear that the meteorological regime approach exposes regime differences between the models and observations that go undetected when using top-level diagnostics. This information can be useful information for developers to better understand model behavior and the influence of parameterization changes. The sensitivity of climate simulations to the representation of clouds under specific meteorological conditions has not been systematically explored and the importance of accurate modeling of clouds under infrequently occurring conditions is unclear. A meteorological regime specific cloud-locking experiment may provide insight into this question.

## 5. Conclusion

In closing, this paper explores the contributions of individual parameterization package updates to changes in Arctic low cloud properties between the two versions of the HadGEM3 atmospheric model (GA6 and GA7.1) using a suite of model experiments. We find that the effect of changing a parameterization depends upon the meteorological regime and that there are often compensating changes between regimes. However, the largest changes in cloud properties can be attributed to single individual parameterizations schemes: low cloud amount to the large-scale cloud scheme, cloud liquid water to the cloud microphysics scheme, and cloud ice concentration to the radiation scheme. Multiple parameterizations contribute to differences in LW and SW CRE between model versions with a substantial contribution from changes in clear-sky fluxes from both the cloud and non-cloud parameterization changes. The results indicate that the parameterization changes have different influences on the meteorological regime independent, regime dependent, and regime frequency change contributions to the cloud property differences.

We conclude that the regime decomposition approach, showing contributions from different meteorological regimes, is useful for model evaluation against observations and when trying to understand changes between model versions and when assessing the regimes that should be

targeted by observations. The regime approach highlights that domain averaged changes in cloud properties due to parameterization changes or under climate change can strongly depend upon the meteorological regime. The results indicate that processes that do not directly influence the cloud properties but influence the regime frequency of occurrence and/or the regime thermodynamic properties are also found to influence the domain average cloud properties and model biases. Lastly, the regime decomposition approach provides a more complete view of the model-simulated cloud response to a parameterization change highlighting the impacts of a parameterization change under conditions that are do not frequently occur and are often overlooked or missed by conventional model diagnostics.

### ***Acknowledgements***

PCT and RCB are supported by the NASA Interdisciplinary Studies Program Grant 80NSSC21K0264 and the NASA Radiation Budget Science Project. ABS was supported by the Met Office Hadley Centre Climate Programme funded by DSIT.

### **Open Research**

*Data Availability Statement:* CERES SYN Ed4a radiative fluxes and cloud properties data (NASA/LARC/SD/ASDC; 2017) are freely available and can be accessed at [asdc.larc.nasa.gov](https://asdc.larc.nasa.gov). MERRA-2 (GMAO 2015) data are available at the GES DISC (<https://disc.gsfc.nasa.gov/datasets?project=MERRA-2>).

## 6. References

- Alkama, R., Cescatti, A., Taylor, P. C., Garcia-San Martin, L., Douville, H., Duveiller, G., et al. (2020). Clouds damp the radiative impacts of polar sea ice loss. *The Cryosphere*, 14, 2673–2686. <https://doi.org/10.5194/tc-14-2673-2020>
- Barahona, D., Molod, A., Bacmeister, J., Nenes, A., Gettelman, A., Morrison, H., Phillips, V., and Eichmann, A. (2014), Development of two-moment cloud microphysics for liquid and ice within the NASA Goddard Earth Observing System Model (GEOS-5), *Geosci. Model Dev.*, 7, 1733–1766, <https://doi.org/10.5194/gmd-7-1733-2014>.
- Baran, A. J., Hill, P., Walters, D., Hardman, S. C., Furtado, K., Field, P. R., and Manners, J., 2016: The impact of two coupled cirrus microphysics-radiation parameterizations on the temperature and specific humidity biases in the tropical tropopause layer in a climate model, *J. Climate*, 29, 5299–5316, <https://doi.org/10.1175/JCLI-D-15-0821.1>.
- Barton, N. P., Klein, S. A., Boyle, J. S., & Zhang, Y. Y. (2012). Arctic synoptic regimes: Comparing domain-wide Arctic cloud observations with CAM4 and CAM5 during similar dynamics. *Journal of Geophysical Research*, 117, D15205. <https://doi.org/10.1029/2012JD017589>
- Bodas-Salcedo, A., and Coauthors, 2011: COSP: Satellite simulation software for model assessment. *Bull. Amer. Meteor. Soc.*, 92, 1023–1043, <https://doi.org/10.1175/2011BAMS2856.1>.
- Bodas-Salcedo, A., Mulcahy, J. P., Andrews, T., et al. (2019). Strong dependence of atmospheric feedbacks on mixed-phase microphysics and aerosol-cloud interactions in HadGEM3. *Journal of Advances in Modeling Earth Systems*, 11, 1735–1758. <https://doi.org/10.1029/2019MS001688>.
- Boeke, R. C. and P. C. Taylor (2016), Evaluation of the Arctic surface radiation budget in CMIP5 models. *J. Geophys. Res.*, **121**, 8525–8548, doi: 10.1002/2016JD025099.
- Boeke, R. C. and Taylor, P. C. (2018). Seasonal energy exchange in sea ice retreat regions contributes to differences in projected Arctic warming. *Nature Communications* **9**, 5017.
- Boutle, I. A. and Abel, S. J. (2012), Microphysical controls on the stratocumulus topped boundary-layer structure during VOCALS-REx, *Atmos. Chem. Phys.*, 12, 2849–2863, <https://doi.org/10.5194/acp-12-2849-2012>, 2012.
- Boutle, I. A., Abel, S. J., Hill, P. G., and Morcrette, C. J. (2014), Spatial variability of liquid cloud and rain: observations and microphysical effects, *Q. J. Roy. Meteorol. Soc.*, 140, 583–594, <https://doi.org/10.1002/qj.2140>.
- Ceppi, P., and P. Nowack (2021). Observational evidence that cloud feedback amplifies global warming. *Proceed. Natl. Acad. Sci.*, **118**(30) e2026290118, doi: <http://doi.org/10.1073/pnas.2026290118>.

Chylek, P., Folland, C., Klett, J. D., Wang, M., Hengartner, N., Lesins, G., & Dubey, M. K. (2022). Annual mean Arctic Amplification 1970–2020: Observed and simulated by CMIP6 climate models. *Geophysical Research Letters*, 49, e2022GL099371. <https://doi.org/10.1029/2022GL099371>

Cohen, J. and coauthors (2020), Divergent consensus on Arctic amplification influence on midlatitude severe winter weather. *Nat. Clim. Chang.* **10**, 20–29, <https://doi.org/10.1038/s41558-019-0662-y>.

Cotton, R. J., Field, P. R., Ulanowski, Z., Kaye, P. H., Hirst, E., Greenaway, R. S., Crawford, I., Crosier, J., and Dorsey, J. (2013), The effective density of small ice particles obtained from in situ aircraft observations of mid-latitude cirrus, *Q. J. Roy. Meteorol. Soc.*, 139, 1923–1934, <https://doi.org/10.1002/qj.2058>.

Curry, J. A., Schramm, J. L., Rossow, W. B., & Randall, D. (1996). Overview of Arctic cloud and radiation characteristics. *Journal of Climate*, 9(8), 1731–1764. [https://doi.org/10.1175/1520-0442\(1996\)009<1731:OOACAR>2.0.CO;2](https://doi.org/10.1175/1520-0442(1996)009<1731:OOACAR>2.0.CO;2)

Doelling, D. R., N. G. Loeb, D. F. Keyes, M. L. Nordeen, D. Morstad, C. Nguyen, B. A. Wielicki, D. F. Young, and M. Sun (2013), Geostationary enhanced temporal interpolation for CERES flux products, *J. Atmos. Oceanic Technol.*, 30, 1072–1090, doi:10.1175/JTECH-D-12-00136.1.

Doelling, D. R., M. Sun, L. T. Nguyen, M. L. Nordeen, C. O. Haney, D. F. Keyes, P. E. Mlynchak (2016), Advances in Geostationary-Derived Longwave Fluxes for the CERES Synoptic (SYN1deg) Product, *J. Atmos. Ocean. Techn.*, **33**(3), 503–521. doi: 10.1175/JTECH-D-15-0147.1

Donohoe, A., Blanchard-Wrigglesworth, E., Schweiger, A., and Rasch, P. J. (2020). The Effect of Atmospheric Transmissivity on Model and Observational Estimates of the Sea Ice Albedo Feedback. *J. Clim.* 33 (13), 5743–5765. doi:10.1175/JCLI-D-19-0674.1

Edwards, J. M. and Slingo, A. (1996), Studies with a flexible new radiation code. I: Choosing a configuration for a large-scale model, *Q. J. Roy. Meteorol. Soc.*, 122, 689–719, <https://doi.org/10.1002/qj.49712253107>.

English, J. M., J. E. Kay, A. Gettelman, X. Liu, Y. Wang, Y. Zhang, and H. Chepfer (2014), Contributions of clouds, surface albedo, and mixed-phase ice nucleation schemes to Arctic radiation biases in CAM5. *J. Climate*, **27**, 5174–5197, doi:10.1175/JCLI-D-13-00608.1.

Field, P. R., Heymsfield, A. J., and Bansemer, A. (2007), Snow Size Distribution Parameterization for Midlatitude and Tropical Ice Clouds, *J. Atmos. Sci.*, 64, 4346–4365, <https://doi.org/10.1175/2007JAS2344.1>, 2007.

Field, P. R., Hill, A. A., Furtado, K., and Korolev, A. (2014), Mixed-phase clouds in a turbulent environment. Part 2: Analytic treatment, *Q. J. Roy. Meteorol. Soc.*, 140, 870–880, <https://doi.org/10.1002/qj.2175>.

Furtado, K., Field, P. R., Boutle, I. A., Morcrette, C. J., and Wilkinson, J. M. (2016), A physically based subgrid parameterization for the production and maintenance of mixed-phase clouds in a general circulation model, *J. Atmos. Sci.*, **73**, 279–291, <https://doi.org/10.1175/JAS-D-15-0021.1>.

Gelaro, R., and coauthors (2017), The Modern-Era Retrospective Analysis for Research and Applications, Version 2 (MERRA-2). *J. Climate*, **30**, 5419-5454, <https://doi.org/10.1175/JCLI-D-16-0758.1>.

Gettelman, A., X. Liu, S. J. Ghan, H. Morrison, S. Park, A. J. Conley, S. A. Klein, J. Boyle, D. L. Mitchell, and J.-L. F. Li (2010), Global simulations of ice nucleation and ice supersaturation with an improved cloud scheme in the Community Atmosphere Model, *J. Geophys. Res.*, **115**, D18216, doi:10.1029/2009JD013797.

Global Modeling and Assimilation Office (GMAO) (2015), *tavg1\_2d\_rad\_Nx: MERRA-2 3D IAU State, Meteorology Instantaneous 1-hourly (p-coord, 0.625x0.5L42), version 5.12.4*, Greenbelt, MD, USA: Goddard Space Flight Center Distributed Active Archive Center, Last accessed 3/23/2023 at doi:10.5067/Q9QMY5PBNV1T.

Hahn L.C., Armour K.C., Zelinka M.D., Bitz C.M. and Donohoe A. (2021), Contributions to Polar Amplification in CMIP5 and CMIP6 Models. *Front. Earth Sci.* **9**:710036. doi: 10.3389/feart.2021.710036

Hill, P. G., Morcrette, C. J., and Boutle, I. A. (2015), A regime-dependent parametrization of subgrid-scale cloud water content variability, *Q. J. Roy. Meteorol. Soc.*, **141**, 1975–1986, <https://doi.org/10.1002/qj.2506>.

Huang, Y. P. C. Taylor, D. Rutan, F. Rose, M. Shupe (2022), Toward a more realistic representation of surface albedo in NASA CERES-derived surface radiative fluxes: A comparison with MOSAIC field campaign, *Elem. Sci. Anth.*, **10**:1, <https://doi.org/10.1515/elementa.2022.00013>.

Jianfen Wei, Zhaomin Wang, Mingyi Gu, Jing-Jia Luo, Yunhe Wang. An evaluation of the Arctic clouds and surface radiative fluxes in CMIP6 models[J]. *Acta Oceanologica Sinica*, 2021, 40(1): 85-102. doi: [10.1007/s13131-021-1705-6](https://doi.org/10.1007/s13131-021-1705-6)

Kato, S., Sun-Mack, S., Miller, W. F., Rose, F. G., Chen, Y., Minnis, P., & Wielicki, B. A. (2010). Relationships among cloud occurrence frequency, overlap, and effective thickness derived from CALIPSO and CloudSat merged cloud vertical profiles, *Journal of Geophysical Research*, **115**, D00H28, doi:10.1029/2009JD012277.

Kato, S., Rose, F. G., Sun-Mack, S., Miller, W. F., Chen, Y., Rutan, D. A., et al. (2011). Improvements of top-of-atmosphere and surface irradiance computations with CALIPSO-, CloudSat-, and MODIS-derived cloud and aerosol properties. *Journal of Geophysical Research*, **116**, D19209. <https://doi.org/10.1029/2011JD016050>

- Kay, J. E., and Gettelman, A. (2009). Cloud influence on and response to seasonal Arctic sea ice loss. *Journal of Geophysical Research*, 114, D18204. <https://doi.org/10.1029/2009JD011773>
- Kay, J. E., and coauthors (2012), Exposing global cloud biases in the community atmosphere model (CAM) using satellite observations and their corresponding instrument simulators. *J. Climate*, **25**, 5190-5207. <https://doi.org/10.1175/JCLI-D-11-00469.1>.
- Klaus, D., K. Dethloff, W. Dorn, A. Rinke, and D. L. Wu (2016), New insight of Arctic cloud parameterization from regional climate model simulations, satellite-based, and drifting station data, *Geophys. Res. Lett.*, 43, 5450–5459, doi:[10.1002/2015GL067530](https://doi.org/10.1002/2015GL067530).
- Komurcu, M., T. Storelvmo, I. Tan, U. Lohmann, Y. Yun, J. E. Penner, Y. Wang, X. Liu, and T. Takemura (2014), Intercomparison of the cloud water phase among global climate models, *J. Geophys. Res. Atmos.*, 119, 3372–3400, doi:[10.1002/2013JD021119](https://doi.org/10.1002/2013JD021119).
- Li, Y. D. W. J. Thompson and S. Bony (2015), The influence of atmospheric cloud radiative effects on the large-scale atmospheric circulation. *J. Climate*, **28**, 7263-7278, <https://doi.org/10.1175/JCLI-D-14-00825.1>.
- Liu, Z. and Schweiger, A. (2017). Synoptic Conditions, Clouds, and Sea Ice Melt Onset in the Beaufort and Chukchi Seasonal Ice Zone, *Journal of Climate*, 30(17), 6999-7016. Retrieved May 24, 2022, from <https://journals.ametsoc.org/view/journals/clim/30/17/jcli-d-16-0887.1.xml>
- Loeb, N. G., and coauthors (2020), Toward a consistent definition between satellite and model clear-sky radiative fluxes. *J. Climate*, **33**, 61-75, <https://doi.org/10.1175/JCLI-D-19-0381.1>.
- Manners, J., Edwards, J. M., Hill, P., and Thelen, J.-C. (2015), SOCRATES (Suite Of Community Radiative Transfer codes based on Edwards and Slingo) Technical Guide, Met Office, UK, available at: <https://code.metoffice.gov.uk/trac/socrates> (last access: 12 October 2023).
- McGraw, Z., Storelvmo, T., Polvani, L. M., Hofer, S., Shaw, J. K., & Gettelman, A. (2023). On the links between ice nucleation, cloud phase, and climate sensitivity in CESM2. *Geophysical Research Letters*, 50, e2023GL105053. <https://doi.org/10.1029/2023GL105053>
- Medeiros, B., Shaw, J., Kay, J. E., & Davis, I. (2023). Assessing clouds using satellite observations through three generations of global atmosphere models. *Earth and Space Science*, 10, e2023EA002918. <https://doi.org/10.1029/2023EA002918>.
- Molod, A. (2012), Constraints on the profile of total water PDF in AGCMs from AIRS and a high-resolution model. *J. Climate*, **25**, 8341-8352, <https://doi.org/10.1175/JCLI-D-11-00412.1>.
- Molod, A., Takacs, L., Suarez, M., and Bacmeister, J. (2015), Development of the GEOS-5 atmospheric general circulation model: evolution from MERRA to MERRA2, *Geosci. Model Dev.*, 8, 1339–1356, <https://doi.org/10.5194/gmd-8-1339-2015>.

- Morcrette, C.J. (2012), Improvements to a prognostic cloud scheme through changes to its cloud erosion parametrization. *Atmosph. Sci. Lett.*, **13**, 95-102. <https://doi.org/10.1002/asl.374>
- Morrison, H., G. de Boer, G. Feingold, J. Harrington, M. D. Shupe, and K. Sulia (2012), Resilience of persistent Arctic mixed-phase clouds, *Nat. Geosci.*, **5**, 11–17, doi:10.1038/ngeo1332.
- Morrison, A. L., Kay, J. E., Chepfer, H., Guzman, R., & Yettella, V. (2018). Isolating the liquid cloud response to recent Arctic sea ice variability using spaceborne lidar observations. *Journal of Geophysical Research: Atmospheres*, **123**, 473–490. <https://doi.org/10.1002/2017JD027248>
- Mulcahy, J. P., Jones, C., Sellar, A., et al. (2018), Improved aerosol processes and effective radiative forcing in HadGEM3 and UKESM1. *Journal of Advances in Modeling Earth Systems*, **10**, 2786–2805. <https://doi.org/10.1029/2018MS001464>.
- NASA/LARC/SD/ASDC (2017). CERES and GEO-enhanced TOA, within-atmosphere and surface fluxes, clouds and aerosols 1-hourly terra-aqua Edition4A. NASA Langley Atmospheric Science Data Center DAAC. [https://asdc.larc.nasa.gov/project/CERES/CER\\_SYN1deg-1Hour\\_Terra-Aqua-MODIS\\_Edition4](https://asdc.larc.nasa.gov/project/CERES/CER_SYN1deg-1Hour_Terra-Aqua-MODIS_Edition4).
- Pithan, F., Medeiros, B. & Mauritsen, T. (2014), Mixed-phase clouds cause climate model biases in Arctic wintertime temperature inversions. *Clim Dyn* **43**, 289–303. <https://doi.org/10.1007/s00382-013-1964-9>.
- Previdi, M., K. L. Smith, L. M. Polvani (2021). Arctic amplification of climate change: A review of underlying mechanisms. *Environ. Res. Lett.*, **16**, 093003, doi: 10.1017/1748-9326/ac1c29.
- Rantanen, M., Karpechko, A.Y., Lipponen, A. *et al.* (2022). The Arctic has warmed nearly four times faster than the globe since 1979. *Commun Earth Environ.*, **3**, 168. <https://doi.org/10.1038/s43247-022-00498-3>
- Rutan, DA, Kato, S, Doelling, DR, Rose, FG, Nguyen, LT, Caldwell, TE, Loeb, NG. 2015. CERES synoptic product: Methodology and validation of surface radiant flux. *Journal of Atmospheric and Oceanic Technology* **32**(6): 1121-1143.
- Segal Rozenhaimer, M., Barton, N., Redemann, J., Schmidt, S., LeBlanc, S., Anderson, B., et al. (2018). Bias and sensitivity of boundary layer clouds and surface radiative fluxes in MERRA-2 and airborne observations over the Beaufort Sea during the ARISE campaign. *Journal of Geophysical Research: Atmospheres*, **123**, 6565–6580. <https://doi.org/10.1029/2018JD028349>
- Sledd, A., and L'Ecuyer, T. S. (2021). Emerging trends in Arctic solar absorption. *Geophysical Research Letters*, **48**, e2021GL095813. <https://doi.org/10.1029/2021GL095813>.
- Sledd, A., L'Ecuyer, T. (2019). How much do clouds mask the impacts of Arctic sea ice and snow cover variations? Different perspectives from observations and reanalyses. *Atmosphere*, **10**(1),12. <https://doi.org/10.3390/atmos10010012>

- Shupe, M. D., Persson, P. O. G., Brooks, I. M., Tjernstrom, M., Sedlar, J., Mauritsen, T., et al. (2013). Cloud and boundary layer interactions over the Arctic sea ice in late summer. *Atmospheric Chemistry and Physics*, 13, 9379-9399. <https://doi.org/10.5194/acp-13-9379-2013>
- Soden, B. J., I. M. Held, R. Colman, K. M. Shell, J. T. Kiehl, and C. A. Shields (2008), Quantifying climate feedbacks using radiative kernels. *J. Climate*, **21**, 3504-3520, <https://doi.org/10.1175/2007JCLI2110.1>.
- Sohn, B.-J., J. Schmetz, R. Stuhlmann, and J.-Y. Lee (2006), Dry bias in satellite-derived clear-sky water vapor and its contribution to longwave cloud radiative forcing. *J. Climate*, **19**, 5570–5580, <https://doi.org/10.1175/JCLI3948.1>.
- Solomon, A., M. D. Shupe, P. O. G. Persson, and H. Morrison (2011), Moisture and dynamical interactions maintaining decoupled Arctic mixed phase stratocumulus in the presence of a humidity inversion, *Atmos. Chem. Phys.*, 11, 10,127–10,148, doi:10.5194/acp-11-10127-2011.
- Solomon, A., et al. (2014), The sensitivity of springtime Arctic mixed-phase stratocumulus clouds to surface-layer and cloud-top inversion layer moisture sources, *J. Atmos. Sci.*, 71, 574–595.
- Stramler, K., A. D. Del Genio, and W. B. Rossow (2011), Synoptically driven Arctic winter states. *J. Climate*, **24**, 1747-1762, <https://doi.org/10.1175/2010JCLI3817.1>.
- Tan, I., and Storelvmo, T. (2019). Evidence of strong contributions from mixed-phase clouds to Arctic climate change. *Geophysical Research Letters*, 46(5), 2894-2902. <https://doi.org/10.1029/2018GL081871>
- Tan, I. and D. Barahona (2022), The impacts of immersion ice nucleation parametrizations on Arctic mixed-phase stratiform cloud properties and the Arctic radiation budget in GEOS-5. *J. Climate*, **35**, 4049-4070. <http://doi.org/10.1175/JCLI-D-21-0368.1>.
- Tan, I., Sotiropoulou, G., Taylor, P.C., Zamora, L. and Wendisch, M. (2023). A Review of the Factors Influencing Arctic Mixed-Phase Clouds: Progress and Outlook. In *Clouds and Their Climatic Impacts* (eds S.C. Sullivan and C. Hoose). <https://doi.org/10.1002/9781119700357.ch5>.
- Taylor, P. C., Kato, S., Xu, K.-M., & Cai, M. (2015). Covariance between Arctic sea ice and clouds within atmospheric state regimes at the satellite footprint level. *Journal of Geophysical Research: Atmospheres*, 120(24), 12656–12678. <https://doi.org/10.1002/2015JD023520>
- Taylor, P. C., W. Maslowski, J. Perlwitz, and D. J. Wuebbles (2017). Arctic Changes and their Effects on Alaska and the Rest of the United States. In: *Climate Science Special Report: Fourth National Climate Assessment, Volume I* [Wuebbles, D. J., S. W. Fahey, K. A. Hibbard, D. J. Dokken, B. C. Steward, and T. K. Maycock (eds.)]. U.S. Global Climate Change Research Program, Washington, DC, USA, pp. 303-332, doi: 10.7930/J00863GK.

Taylor, P. C., R. C. Boeke, Y. Li, and D. W. J. Thompson (2019). Arctic cloud annual cycle biases in climate models, *Atmos. Chem. Phys.*, **19**, 8759–8782, <https://doi.org/10.5194/acp-19-8759-2019>.

Taylor P. C., Boeke R. C., Boisvert L. N, Feldl N., Henry M., Huang Y., Langen P. L., Liu W., Pithan F., Sejas S. A. and Tan I. (2022). Process Drivers, Inter-Model Spread, and the Path Forward: A Review of Amplified Arctic Warming. *Front. Earth Sci.* 9:758361. doi: 10.3389/feart.2021.758361

Taylor, P. C., and E. Monroe (2023), Isolating the surface type influence on Arctic low-clouds. *Journal of Geophysical Research: Atmospheres*, 128, e2022JD038098. <https://doi.org/10.1029/2022JD038098>

Tselioudis, G. and coauthors (2021), Evaluation of clouds, radiation, and precipitation in CMIP6 models using global weather state derived from ISCCP-H cloud property data. *J. Climate*, **34**, 7311–7324, <https://doi.org/10.1175/JCLI-D-21-0076.1>.

Van Weverberg, K., Boutle, I. A., Morcrette, C. J., and Newsom, R. K. (2016), Towards retrieving critical relative humidity from ground-based remote-sensing observations, *Q. J. Roy. Meteorol. Soc.*, 142, 2867–2881, <https://doi.org/10.1002/qj.2874>.

Vihma, T., Pirazzini, R., Fer, I., Renfrew, I. A., Sedlar, J., Tjernström, M., et al. (2014). Advances in understanding and parameterization of small-scale physical processes in the marine Arctic climate system: A review. *Atmospheric Chemistry and Physics*, 14, 9403–9450. <https://doi.org/10.5194/acp-14-9403-2014>

Voigt A, Albern N, Ceppi P, Grise K, Li Y, Medeiros B (2021), Clouds, radiation, and atmospheric circulation in the present-day climate and under climate change. *WIREs Clim Change*, Voigt A, Albern N, Ceppi P, Grise K, Li Y, Medeiros B. Clouds, radiation, and atmospheric circulation in the present-day climate and under climate change. *WIREs Clim Change*. 2021; 12:e694. <https://doi.org/10.1002/wcc.694> (e694), <https://doi.org/10.1002/wcc.694>.

Walters, D., Baran, A. J., Boutle, I., et al. (2019), The Met Office Unified Model Global Atmosphere 7.0/7.1 and JULES Global Land 7.0 configurations, *Geosci. Model Dev.*, 12, 1909–1963, <https://doi.org/10.5194/gmd-12-1909-2019>.

Wilson, D. R., Bushell, A. C., Kerr-Munslow, A. M., Price, J. D., and Morcrette, C. J. (2008a), PC2: A prognostic cloud fraction and condensation scheme. I: Scheme description, *Q. J. Roy. Meteorol. Soc.*, 134, 2093–2107, <https://doi.org/10.1002/qj.333>, 2008a.

Wilson, D. R., Bushell, A. C., Kerr-Munslow, A. M., Price, J. D., Morcrette, C. J., and Bodas-Salcedo, A. (2008b), PC2: A prognostic cloud fraction and condensation scheme. II: Climate model simulations, *Q. J. Roy. Meteorol. Soc.*, 134, 2109–2125, <https://doi.org/10.1002/qj.332>.

Yeo, H., M.-H. Kim, S.-W. Son, J.-H. Jeong, J.-H. Yoon, B.-M. Kim, S.-W. Kim (2022), Arctic cloud properties and associated radiative effects in the three newer reanalysis datasets (ERA5, MERRA-2, JRA-55): Discrepancies and possible causes, *Atmos. Res.*, **270**, <https://doi.org/10.1016/j.atmosres.2022.106080>.

Yu, Y., Taylor, P. C., & Cai, M. (2019). Seasonal variations of Arctic low-level clouds and its linkage to sea ice seasonal variations. *Journal of Geophysical Research: Atmospheres*, 124(2), 12206-12226. <https://doi.org/10.1029/2019JD031014>

Zelinka, M. D., Myers, T. A., McCoy, D. T., Po-Chedley, S., Caldwell, P. M., Ceppi, P., et al. (2020). Causes of higher climate sensitivity in CMIP6 models. *Geophysical Research Letters*, 47, e2019GL085782. <https://doi.org/10.1029/2019GL085782>.

Zelinka, M.D., and coauthors (2023), Detailing cloud property feedbacks with a regime-based decomposition. *Clim Dyn.*, **60**, 2983–3003, <https://doi.org/10.1007/s00382-022-06488-7>.

# **Influence of parameterization changes on Arctic low cloud properties and cloud radiative effects in two versions of the HadGEM3 Atmospheric Model: GA7.1 and GA6**

Patrick C. Taylor<sup>1,\*</sup>, Robyn C. Boeke<sup>2</sup>, Alejandro Bodas-Salcedo<sup>3</sup>

<sup>1</sup>NASA Langley Research Center, Hampton, VA, USA

<sup>2</sup>Analytical Mechanical Associates, Hampton, VA, USA

<sup>3</sup>Met Office Hadley Centre, Exeter, UK

## Key Messages:

- Individual parameterization changes explain cloud property changes and multiple parameterizations explain cloud radiative effect changes.
- The large-scale cloud scheme is the single most impactful parameterization to changes in Arctic meteorological regime frequency.
- Non-cloud parameterizations must be considered to understand the full influence of parameterization changes on cloud radiative effects.

\*Corresponding author email: [patrick.c.taylor@nasa.gov](mailto:patrick.c.taylor@nasa.gov)

## Abstract

Arctic clouds play a key role in Arctic climate variability and change; however, contemporary climate models struggle to simulate cloud properties accurately. Model-simulated cloud properties are determined by the physical parameterizations and their interactions within the model configuration. Quantifying effects of individual parameterization changes on model-simulated clouds informs efforts to improve cloud properties in models and provides insights on climate system behavior. This study quantifies the influence of individual parameterization schemes on Arctic low cloud properties within the Hadley Centre Global Environmental Model 3 atmospheric model using a suite of experiments where individual parameterization packages are changed one-at-a-time between two configurations: GA6 and GA7.1. The results indicate that individual parameterization changes explain most of the cloud property differences, whereas multiple parameterizations, including non-cloud schemes, contribute to cloud radiative effect differences. The influence of a parameterization change on cloud properties is found to vary by meteorological regime. We employ a three-term decomposition to quantify contributions from (1) regime independent, (2) regime dependent, and (3) the regime frequency of occurrence changes. Decomposition results indicate that each term contributes differently to each cloud property change and that non-cloud parameterization changes make a substantial contribution to the LW and SW cloud radiative effects by modifying clear-sky fluxes differently across regimes. The analysis provides insights on the role of non-cloud parameterizations for setting cloud radiative effects, a model pathway for cloud-atmosphere circulation interactions, and raises questions on the most useful observational approaches for improving models.

## **Plain Language Summary**

Arctic clouds play a key role in Arctic climate variability and change; however, state-of-the-art climate models struggle to simulate cloud properties accurately. Errors in model-simulated cloud have known and unknown influences on the simulated climate state and climate change projections. Model cloud properties are determined by the physical parameterizations and their interactions within the model. Thus, to improve model-simulated clouds, we need to understand the effects of parameterization changes. We use a series of Hadley Centre Global Environmental Model 3 atmospheric model simulations where individual parameterizations are changed one-at-a-time. This approach allows us to isolate the influence of individual cloud parameterizations on model-simulated cloud properties to inform model development and the observations needed to improve models. The results show that individual parameterizations are most important for specific cloud variables and that multiple parameterizations are important to determining the model-simulated influence of clouds on the energy budget. We also find that changes in model-simulated cloud properties respond differently under different weather conditions. The analysis provides insights on the role of non-cloud parameterizations for setting cloud radiative effects, the ways that clouds and the atmosphere interact, and raises questions on the most useful observational approaches for improving models.

## 1. Introduction

The Arctic is rapidly changing; observed and simulated surface temperature trends are larger than any other region (e.g., Taylor et al. 2017; Chylek et al. 2021; Rantanen et al. 2022). Climate change simulations point to an acceleration of Arctic warming through the 21<sup>st</sup> century; however, the climate model projected warming rate has a large inter-model spread (e.g., Previdi et al. 2021; Taylor et al. 2022). Narrowing the spread in future predictions is a key scientific challenge requiring improved knowledge of the processes driving Arctic change.

Cloud feedbacks are an important factor in global and Arctic climate change (Zelinka et al. 2020; Ceppi et al. 2021; Hahn et al. 2021; Tan et al. 2023; McGraw et al. 2023). A change in Arctic cloud properties in response to surface warming can affect the Arctic climate system by modulating the thermodynamic structure of the Arctic atmosphere, altering the surface energy budget, masking the radiative response of sea ice loss, and changing the mass balance of Arctic sea ice (Curry et al. 1996; Vihma et al. 2014; Tan et al. 2019; Sledd and L'Ecuyer 2019; Alkama et al. 2020; Sledd and L'Ecuyer 2021). The magnitude of Arctic cloud feedback varies substantially across contemporary climate models and impacts the projection of Arctic warming and sea ice loss (e.g., Boeke and Taylor 2018; Hahn et al. 2021; Tan et al. 2019). Thus, a better representation of Arctic cloud properties and evolution within climate models will help narrow the spread in Arctic cloud feedback and climate change projections.

Recent studies highlight model-observational discrepancies in Arctic cloud properties and indicate that model-simulated cloud biases stem from multiple sources. In Coupled Model Intercomparison Project 5 (CMIP5) models, Boeke and Taylor (2016) show that model-simulated clouds are too reflective in summer and not insulating enough in winter. These errors in the cloud radiative effects are related to too little cloud amount, too little cloud liquid, too much cloud ice,

and errors in the seasonal evolution of cloud properties (e.g., Komurcu et al. 2014; Klaus et al. 2016; Taylor and Boeke 2016; Taylor et al. 2019). These model-observational differences in CMIP5 models generally remain in CMIP6 (e.g., Tselioudis et al. 2021). Cloud microphysical and aerosol parameterizations strongly affect model-simulated cloud properties and radiative effects but are not the only contributing factors (e.g., Gettelman et al. 2010; Komurcu et al. 2014; English et al. 2014; Taylor et al. 2015; Klaus et al. 2016; Morrison et al. 2018; Taylor et al. 2019; Tan and Barahona 2022; Tan et al. 2023). Pithan et al. (2014) explore ‘clear’ and ‘cloudy’ states of the Arctic wintertime boundary layer finding that the transition between mixed phase and ice clouds is not only a function of cloud microphysics, but also a result of a change in meteorological regimes and dynamical interactions. This suggests that the frequency of meteorological regimes can also substantially influence model-simulated cloud properties (e.g., Stramler et al. 2011; Morrison et al. 2012). These results underscore the importance of understanding the influence of specific parameterizations on simulated cloud properties and the dependence on meteorological regime.

This study aims to advance our understanding of the multiple influences on model-simulated Arctic low cloud properties. The experimental approach employed uses simulations from two consecutive configurations of the atmospheric component of the Hadley Centre Global Environmental Model (HadGEM) GA6 and GA7.1. This study leverages HadGEM3 cloud parameterization experiments from Bodas-Salcedo et al. (2019) that individually turn on/off parameterization package updates between GA6 and GA7.1 to assess the influence of each on simulated Arctic cloud properties. The study stratifies cloud properties and radiative effects by meteorological regimes, following Taylor et al. (2019), to investigate the dependence of the cloud property response to parameterization changes on meteorological conditions. The results are compared to Clouds and the Earth’s Radiant Energy System (CERES) observations and the

Modern-Era Retrospective analysis for Research and Applications-2 (MERRA-2). The study objective is to determine the most important parameterizations affecting Arctic cloud properties in HadGEM3 and evaluate the alignment with observations.

## **2. Model, Data, and Methodology**

### 2.1. Model Description

The analysis uses the two configurations of the HadGEM3 atmosphere model—GA6 and GA7.1. These configurations are set apart by the suite of parameterization updates from GA6 to GA7.1. To make the number of simulations manageable, individual updates are grouped into development “packages”, as in Bodas-Salcedo et al. (2019). A package is a collection of parameterization changes that are related, either because they modify the same physical parameterization (e.g., convection) or because they are logically dependent. A complete list of model changes introduced between GA6 and GA7.1 can be found in Walters et al. (2019) and Mulcahy et al. (2018), and a description of the packages in Bodas-Salcedo et al. (2019). We provide a brief description of the individual package changes that explain most of the differences in the simulation of Arctic clouds between GA7.1 and GA6.

#### 2.1.1. Large-scale cloud

The large-scale cloud scheme is responsible for the calculation of the cloud fraction and condensate within each gridbox at each timestep (Wilson et al. 2008a,b; Morcrette 2012; Van Weverberg et al. 2016). The primary changes in this package are listed below.

- Radiative impact of convective cores: the profiles of convective cloud amount and cloud condensate are combined with the large-scale cloud fields before being passed to the cloud generator of the radiative transfer code.

- Consistent treatment of phase change for convective condensate passed to large-scale cloud: this change enforces consistency between the upper temperature limit at which ice can be formed by convection and in the large-scale cloud scheme.
- Turbulence-based critical relative humidity: the value of the critical relative humidity used to initiate cloud in cloud-free grid boxes or to remove cloud from cloud-filled grid boxes has changed from being constant at each model level to being dependent on sub-grid turbulence.
- Removal of redundant complexity for ice cloud: this removes the effect of two ice cloud fraction increment terms that partially offset and had no clear physical justification.
- A retuning of the low cloud was carried out with the aim of reducing its albedo while maintaining the improved cloud cover.

#### 2.1.2. Radiation

The radiation code updates the vertical profiles of heating rates in each gridbox due to radiative processes in the solar and terrestrial parts of the spectrum (Edwards and Slingo, 1996; Manners et al., 2015). The changes in this package are listed below.

- Consistent ice optical and microphysical properties: update of the parameterization for scalar optical properties of ice crystals to the formulation by Baran et al. (2016).
- Revised ice microphysical properties: the representation of ice particle size distribution is updated to the empirical distribution of Field et al. (2007), and the mass-diameter relation is updated based upon measurements with improved accuracy (Cotton et al. 2013).
- Improved treatment of gaseous absorption: improved representation of H<sub>2</sub>O, CO<sub>2</sub>, O<sub>3</sub> and O<sub>2</sub> absorption in the SW and of all gases in the LW.

#### 2.1.3. Microphysics

This package bundles changes related to large-scale precipitation or strongly coupled to microphysical processes, as listed below.

- Improved treatment of sub-grid-scale cloud water content variability: parameterization of the fractional standard deviation of cloud water content as formulated in Hill et al. (2015).
- New warm rain microphysics: re-write of the warm rain part of the large-scale precipitation scheme, as documented in Boutle and Abel (2012) and Boutle et al. (2014).
- Turbulent production of liquid water in mixed-phase cloud: implementation of a new parameterization of liquid water production in mixed-phase cloud (Field et al. 2014; Furtado et al. 2016).

## 2.2. Model Experiments

The model experiment suite consists of a series of 14-year AMIP-style simulations where the updated development packages are turned on/off individually to target either GA7.1 (using GA6 as a baseline and turning an updated package on) or GA6 (using GA7.1 as a baseline and turning an updated package off). The union of all packages contain all changes between GA6 and GA7.1.

Daily and monthly data are used from March 2000 to December 2014. Due to the large number of parameterization package changes between GA6 and GA7.1, monthly output is used to identify the packages with the greatest effect on monthly mean cloud properties (not shown). Table 1 lists the ten individual parameterizations and two combinations that have the largest impact on monthly mean cloud properties. The analysis described in Section 3 uses daily output from GA6\_ON

experiments; simulations using the base GA6 model where a single parameterization scheme is updated to the GA7.1 parameterization one at a time, hereafter called ON\_experiments.

**Table 1.** Summary of the development packages analyzed.

<b>Name</b>	<b>Parameterization Package</b>
Rad	Radiation
Aer	Aerosols
Mic	Microphysics and large-scale precipitation
Cld	Large-scale cloud
Cnv	Convection
BL	Boundary layer
GWD	Gravity wave drag
Dyn	Dynamics
Sto	Stochastic physics
Lnd	Land surface
AerErf	Aerosols + Effective radiative forcing
MicCldRad	Microphysics and large-scale precipitation + Large-scale cloud + Radiation

### 2.3. Data and Reanalysis

#### 2.3.1. Clouds and Earth’s Radiant Energy System (CERES)

The CERES synoptic edition 4A product (SYN Ed4a, Doelling et al. 2013; 2016) provides 1-hourly radiative fluxes at the surface, four atmospheric levels (850, 500, 200, and 70 hPa), and the top of the atmosphere (TOA) at  $1^\circ \times 1^\circ$  spatial resolution. The in-atmosphere and surface fluxes are computed hourly using the Langley-modified Fu–Liou radiative transfer model using inputs from the Moderate Resolution Imaging Spectroradiometer (MODIS) and meteorological state from the Goddard Earth Observing System Version 5.4.1 (GEOS-5.4.1; Rutan et al., 2015). Cloud properties are retrieved within four layers: low (surface to 700 hPa), middle (700–500 hPa), middle-high (500–300 hPa), and high (300–50 hPa). Cloud radiative effect (CRE) is defined as the difference between all-sky minus clear-sky fluxes in the LW and SW using downwelling fluxes only to minimize the impact of surface albedo differences. Radiative flux uncertainty of  $\pm 12 \text{ W m}^{-2}$  is adopted for clear-sky fluxes and  $\pm 16 \text{ W m}^{-2}$  for all-sky fluxes and CRE following Kato et al.

(2010; 2011). These uncertainty estimates align with a recent comparison between CERES SYN Ed4a and surface radiometer measurements during the Multidisciplinary drifting Observatory for the Study of Arctic Climate (Huang et al. 2022).

### 2.3.2. MERRA-2

MERRA-2 (Gelaro et al. 2017) is the latest reanalysis produced by the Goddard Modeling and Assimilation Office (GMAO). MERRA-2 uses version 5.12.4 of the GEOS atmospheric model and data assimilation system with horizontal resolution of  $0.58^\circ$  latitude by  $0.6258^\circ$  longitude with a vertical resolution of 72 hybrid-eta levels at 1-hourly temporal resolution (Molod et al. 2015). For this study, MERRA-2 cloud liquid and ice water concentration (CLW and CLI, respectively) profiles are compared with the GA6 and GA7.1 (GMAO 2015).

### 2.4. Meteorological Regime Framework

The meteorological regime framework enables the quantification of differences between models and observations and between model experiments on a regimes-by-regime basis. Meteorological regime analysis provides insights into the processes that influence cloud properties

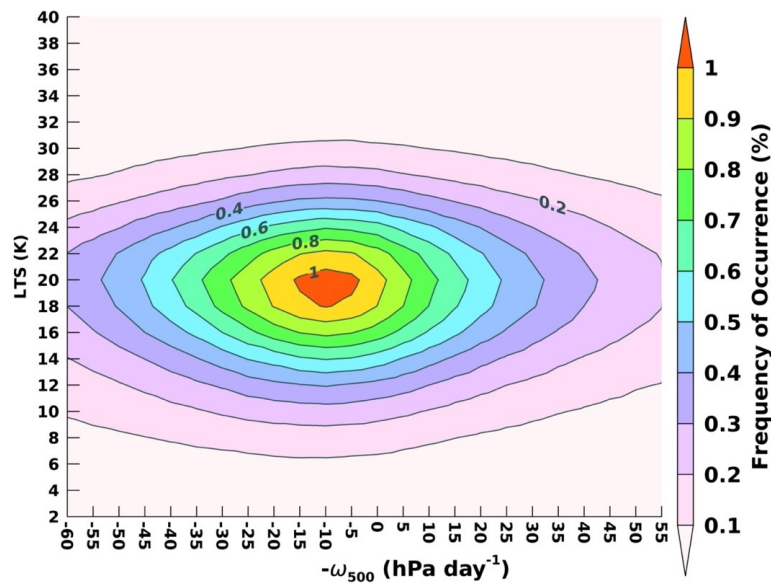


**Figure 1:** Relative frequency of occurrence (RFO) for the meteorological regime phase space of (x-axis) 500 hPa vertical velocity ( $\omega_{500}$ ) and (y-axis) lower tropospheric stability (LTS) for GA6.  $-\omega_{500}$  is used to have ascending motion be represented as a positive number.

under specific atmospheric conditions (e.g., Stramler et al. 2011; Barton et al. 2012; Liu and Schweiger 2017; Taylor et al. 2015; 2019; Zelinka et al. 2023). Studies show that Arctic low cloud amount (LCA) and CLI and CLW are strongly influenced by lower tropospheric stability (LTS) and 500 hPa vertical velocity ( $\omega_{500}$ ) (Solomon et al. 2011; 2014; Shupe et al. 2013; Taylor et al. 2019; Yu et al. 2019; Taylor and Monroe 2023); thus, we stratify cloud properties by these variables to determine regime dependent differences. Figure 1 shows the relative frequency of occurrence (hereafter RFO) of GA6 LTS/ $-\omega_{500}$  meteorological regimes. The most frequent regimes show mid-high stability (LTS  $\sim$  19 K) and weak subsidence ( $-\omega_{500} \sim -10$  hPa day $^{-1}$ ; vertical velocity is expressed  $-\omega_{500}$  for ease of interpretation, positive values indicate rising motion).

Using the RFO and the LCA in each LTS/ $-\omega_{500}$  bin, the average cloud amount can be defined as

$$\overline{LCA} = \sum_{i,j} LCA(LTS_i, -\omega_{500,j}) \cdot RFO(LTS_i, -\omega_{500,j}) \quad (1)$$

where  $LCA(LTS_i, -\omega_{500,j})$  is the average low cloud amount and  $RFO(LTS_i, -\omega_{500,j})$  is the relative frequency of occurrence of the  $i^{\text{th}}$  and  $j^{\text{th}}$  LTS/ $-\omega_{500,j}$  bin. The summation of RFO over all  $i,j$  bins equals one. Applying a first-order Taylor series approximation of (1) and reordering terms allows for the separation of the GA7.1 minus GA6 differences ( $\delta\overline{LCA}_{GA7.1-GA6}$ ) into three terms,

$$\delta\overline{LCA}_{GA7.1-GA6} = \sum_{i,j} \delta LCA'(LTS_i, -\omega_{500,j})_{GA7.1-GA6} \cdot RFO(LTS_i, -\omega_{500,j})_{GA6} + \delta\overline{LCA}_{GA7.1-GA6, equal} \cdot RFO(LTS_i, -\omega_{500,j})_{GA6} + LCA(LTS_i, -\omega_{500,j})_{GA6} \cdot \delta RFO(LTS_i, -\omega_{500,j})_{GA7.1-GA6} \quad (2)$$

where  $\delta\overline{LCA}$  (left-hand side of (2)) is the total difference in LCA between GA7.1 minus GA6. The three terms on the righthand side of (2) from top to bottom represent (a) regime independent, (b) regime dependent, and (c) RFO contributions to total cloud property changes. The regime

independent and dependent terms are determined by defining  $\delta LCA(LTS_i, -\omega_{500,j})_{GA7.1-GA6}$  as the sum of  $\delta \overline{LCA}_{GA7.1-GA6, equal} + \delta LCA'(LTS_i, -\omega_{500,j})_{GA7.1-GA6}$ .

$$\delta \overline{LCA}_{GA7.1-GA6, equal} = \frac{1}{N} \sum_{i,j} \delta LCA(LTS_i, -\omega_{500,j})_{GA7.1-GA6} \quad \text{and} \quad (3)$$

$$\begin{aligned} \delta LCA'(LTS_i, -\omega_{500,j})_{GA7.1-GA6} \\ = \delta LCA(LTS_i, -\omega_{500,j}) - \delta \overline{LCA}_{GA7.1-GA6, equal} \end{aligned} \quad (4).$$

The regime independent term,  $\delta \overline{LCA}_{GA7.1-GA6, equal}$ , represents the equal-weight average cloud property change across all  $LTS_i/-\omega_{500,j}$  bins, where  $N$  is the total number of bins. The regime dependent term,  $\delta LCA'(LTS_i, -\omega_{500,j})_{GA7.1-GA6}$ , represents the deviation of the cloud properties within a regime from the equal-weight averaged GA7.1-GA6 difference across all regimes. The RFO term represents the contributions to the GA7.1-GA6 differences from shifts in regime frequency. Equation (2) is applied to LCA, CLI, CLW, and LW and SW CRE to quantify the relative contributions of these terms to inter-model and model-observation differences.

### 3. Results

#### 3.1. GA7.1 and GA6 differences

This section documents the cloud properties and radiative flux changes between GA6 and GA7.1. To provide a comprehensive perspective of these differences, we present a comparison of the Arctic domain average and meteorological regime average cloud properties.

Table 2 summarizes the Arctic domain average cloud properties and LW and SW CRE for GA6 and differences with GA7.1 and the ON\_experiments (discussed in Section 3b). The final line in Table 2 shows the linear combination of the individual ON\_experiments and AerErf\_ON; MicCldRad\_ON and Aer\_ON are not included in this sum to avoid double counting. This line can be compared to the full difference GA7.1 - GA6 (Table 2, line 2) indicating a greater degree of

closure for cloud property variables than for radiative fluxes. A comparison with observations is provided in Section 3c. Table 2 indicates that GA7.1 has less LCA than GA6 in the annual mean and in each season (not shown). Conversely, GA7.1 shows greater annual mean and seasonal CLI and CLW in the lower atmosphere than GA6.

**Table 2.** Summary of Arctic domain average cloud properties and radiative effects for model simulations, where RLSDSCS, RSDSCS, and RSUSCS represent the downwelling longwave clear-sky flux, the downwelling shortwave clear-sky flux, and the upwelling shortwave clear-sky flux at the surface.

	<i>CA</i> (%)	<i>CLI</i> (g kg <sup>-1</sup> )	<i>CLW</i> (g kg <sup>-1</sup> )	<i>LWCRE</i> (W m <sup>-2</sup> )	<i>RLSDSCS</i> (W m <sup>-2</sup> )	<i>SWCRE</i> (W m <sup>-2</sup> )	<i>RSDSCS</i> (W m <sup>-2</sup> )	<i>RSUSCS</i> (W m <sup>-2</sup> )
<b>GA6</b>	29.70	5.96	5.67	39.66	204.27	-44.71	146.32	58.32
<b>GA7.1-GA6</b>	-6.02	3.33	2.32	2.78	1.14	-0.01	-3.51	-3.95
<i>Rad_ON-GA6</i>	0.72	2.49	0.02	1.17	1.47	0.81	-1.75	-0.99
<i>Aer_ON-GA6</i>	0.30	0.14	-0.11	1.52	-1.95	-1.69	-0.58	-0.08
<i>Mic_ON-GA6</i>	1.07	0.22	1.30	1.05	-1.31	-2.47	0.10	0.18
<i>Cld_ON-GA6</i>	-8.80	-0.63	0.07	-4.17	-2.42	5.66	0.25	0.72
<i>Cnv_ON-GA6</i>	0.61	0.33	-0.18	0.70	-1.47	-1.14	0.24	0.10
<i>BL_ON-GA6</i>	0.23	0.56	-0.04	0.69	0.06	-1.26	0.03	-0.10
<i>GWD_ON-GA6</i>	-0.59	-0.10	-0.18	-0.95	0.13	1.13	-0.04	-0.23
<i>Dyn_ON-GA6</i>	-0.46	-0.07	-0.01	-0.32	-0.34	0.20	-0.06	-0.22
<i>Sto_ON-GA6</i>	-0.08	0.11	-0.02	0.66	0.08	-1.06	-0.06	-0.11
<i>Lnd_ON-GA6</i>	-0.52	-0.02	0.21	0.25	2.98	-0.30	-0.59	-2.75
<i>AerErf_ON-GA6</i>	0.17	0.18	0.03	1.27	-0.63	-0.40	-1.46	-2.41
<i>MicCldRad_ON-GA6</i>	-6.54	1.78	1.26	-1.60	-1.42	4.00	-1.37	0.10
<b>Sum of ON_Experiments</b>	-7.67	3.07	1.19	0.35	-1.43	1.17	-3.35	-5.81
<b>CERES</b>	40.7	--	--	43.8	209.0	-43.1	141.6	46.1
<b>MERRA-2</b>	--	1.12	20.9	--	--	--	--	--

The domain average cloud property changes compete in their influence on LW and SW CRE.

The result shows that GA7.1 has a larger annual mean LW CRE than GA6 and in each season except for June-July-August (not shown). SW CRE shows little change in the annual mean due to offsetting seasonal differences: GA7.1 more negative than GA6 in spring and less negative in summer. GA7.1 has a greater downwelling clear-sky LW flux and less downwelling and upwelling clear-sky SW flux at the surface. The clear-sky flux changes impact the CREs, where the increased

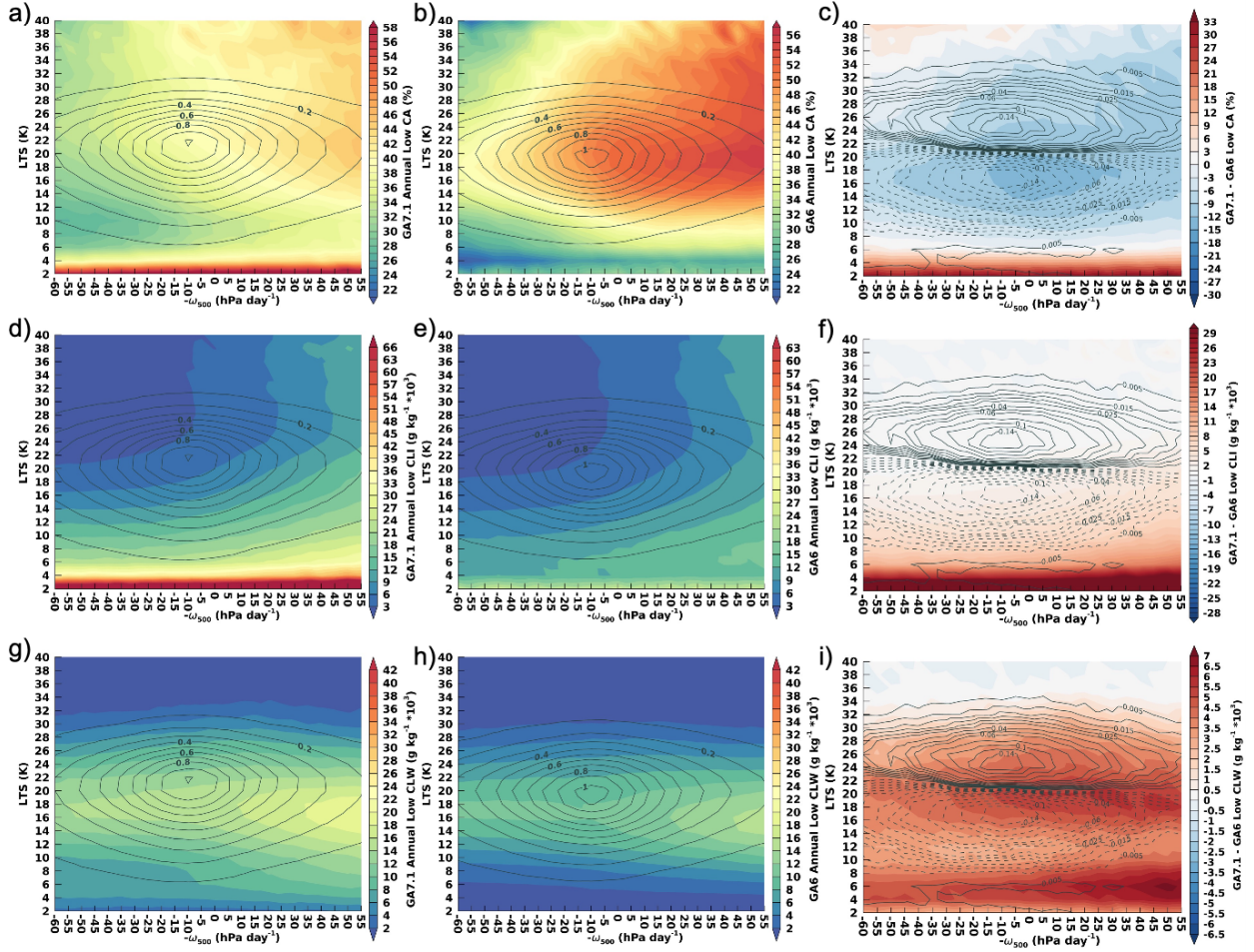


**Figure 2.** Annual mean (a-c) low cloud amount, (d-f) cloud ice mixing ratio (units:  $\text{g kg}^{-1}$ ), and (g-i) cloud liquid mixing ratio (units:  $\text{g kg}^{-1}$ ) within LTS/ $-\omega_{500}$  meteorological regimes for GA7.1, GA6, and GA7.1-GA6 differences, respectively.

downwelling LW clear-sky flux reduces GA7.1 minus GA6 LW CRE difference. In the SW, the reductions in downwelling SW clear-sky fluxes offset the influence of increased CLW and CLI. Overall, Table 2 illustrates substantial changes in domain average cloud properties, CRE, and clear-sky fluxes between GA7.1 and GA6.

We find that domain average changes are not distributed evenly across meteorological regimes. Figure 2 shows the average LCA, CLI, and CLW values within the LTS/ $-\omega_{500}$  regimes for GA7.1, GA6, and the GA7.1 minus GA6 differences. For LCA, the smaller GA7.1 average LCA results from a general reduction in LCA across a range of the most frequently occurring regimes (Fig. 2c); the largest LCA reductions are found in regimes with LTS between 12-20 K and weak to moderate

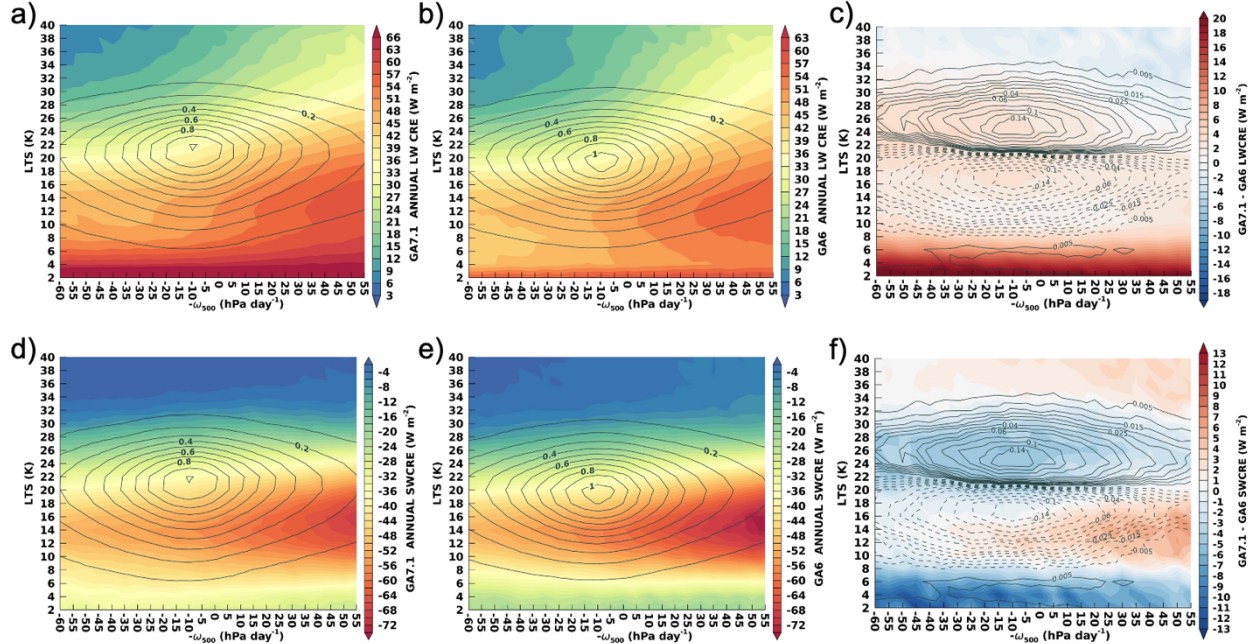


**Figure 3.** Annual mean (a-c) LW CRE and (d-f) SW CRE within LTS/ $\omega_{500}$  meteorological regimes for GA7.1, GA6, and GA7.1-GA6 differences. Units are  $\text{W m}^{-2}$ .

rising motion. Large increases in LCA (exceeding 20%) are found at  $\text{LTS} < 4 \text{ K}$ . However, these LCA increases do not contribute substantially to the domain average due to their low RFO.

Meteorological regime dependent differences between GA7.1 and GA6 are also found for CLI and CLW. The greater domain average CLI in GA7.1 (Fig. 2f) is supported by small increases across many meteorological regimes with the largest increases at  $\text{LTS} < 12 \text{ K}$  (Fig. 2f); these increases show a weak dependence on  $\omega_{500}$ . In contrast, CLW differences between GA7.1 and GA6 vary with  $\omega_{500}$  and the strongest CLW increases occur in regimes of rising motion. The larger domain average GA7.1 CLW is supported by strong increases across a range of LTS values from 2-32 K (Fig. 2i). The meteorological regimes that show the largest increases in CLW also show the largest reductions in LCA. Large increases in CLI and CLW are also found at  $\text{LTS} < 4 \text{ K}$ .

The distribution of LW and SW CRE changes between GA7.1 and GA6 across meteorological regimes result from the competing influences of LCA and CLW changes (Fig. 3). GA7.1 shows greater LW CRE than GA6 across most meteorological regimes with a few meteorological regimes

showing greater increases, including at  $LTS < 8$  K and under moderate subsidence conditions with LTS between 20-28K. For SW CRE, the GA7.1-GA6 differences vary strongly across meteorological regimes; more negative differences are found at  $LTS < 6$  K and between 22-30 K. GA7.1 shows more positive SW CRE than GA6 at LTS between 10-16 K. The results indicate that for regimes where LW CRE increases and SW CRE decreases the CLW increase dominates the CRE change, whereas in the regimes where LW CRE decreases and SW CRE increases the LCA decrease dominates.

Changes in meteorological regime RFO also influence the GA7.1-GA6 differences. The solid and dotted contours in Fig. 2c indicates a RFO shift toward increased LTS in GA7.1 than GA6. This shift reduces the impact of LCA reductions as the regimes with the greatest reductions also have reduced RFOs. Conversely, the CLW increase and the increased LW and SW CRE magnitudes in GA7.1 contribute more strongly to the domain average, as regimes with increased RFO show a greater CLW increase. The RFO changes play a minor role in CLI differences. Clear from Fig. 2 and 3, the domain averaged differences in the cloud properties are influenced by a combination of changes in meteorological regime cloud properties and changes in regime RFO. To quantify the influence of RFO, we apply the decomposition in (2)-(4).

Different terms of the decomposition (Fig. 4) dominate the GA7.1-GA6 differences for different cloud variables. The regime independent term accounts for the largest contribution to the CLI, CLW, and LW CRE differences. For CLI, the regime dependent term partly offsets the regime independent term. The regime dependent term makes the largest contribution to the LCA reduction from GA6 to GA7.1. The RFO term makes the largest contribution to the SW CRE differences.

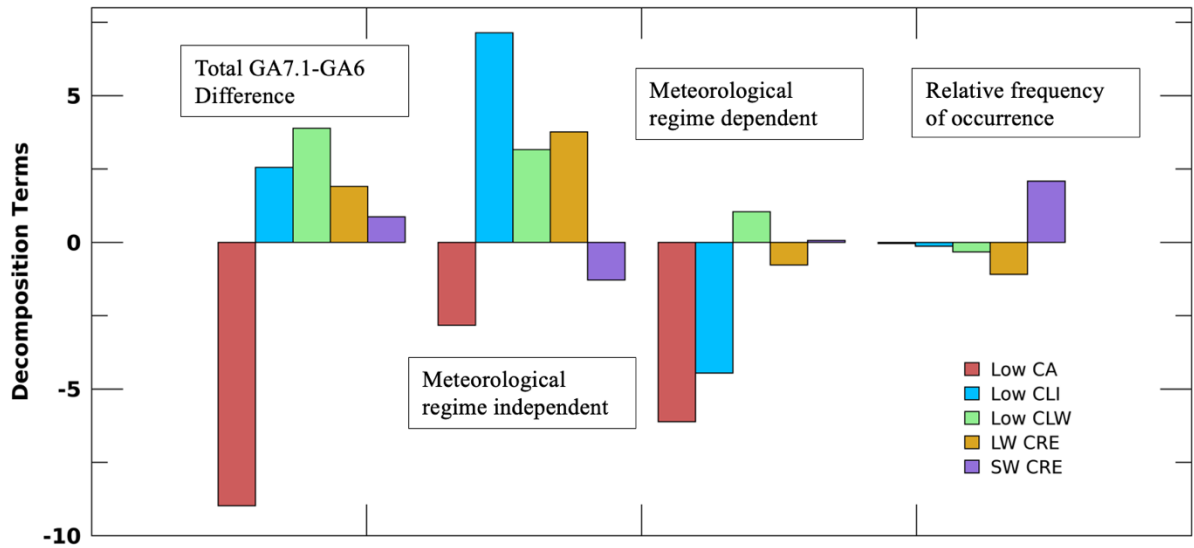


**Figure 4.** Annual mean contributions (units: %,  $\text{g kg}^{-1}$ , and  $\text{Wm}^{-2}$ ) from left to right are the total GA7.1-GA6 difference, meteorological regime independent, meteorological regime dependent, and relative frequency of occurrence contributions to (red) LCA, (blue) CLI, (green) CLW, (gold) LW CRE, and (purple) SW CRE.

The results indicate that when assessing the factors that influence the changes in the cloud and radiative properties one cannot assume that the factors that determine the change in one cloud property also explain the change in another.

### 3.2. Role of individual parameterizations

Many parameterization updates make up the evolution from GA6 to GA7; however, the results show that a handful explain most of the cloud property differences. Using the suite of ON\_experiments (Table 1), we quantify the influence of individual parameterization schemes on the GA7.1 minus GA6 cloud differences. Two of the ON\_experiments are combinations of parameterization scheme changes: AerErf\_ON and MicCldRad\_ON.

The analysis of domain average cloud property and CRE changes for the ON\_experiments indicate that the parameterization packages that most strongly influence the GA7.1-GA6 differences are different for each cloud variable. For cloud properties, the annual mean domain average change from GA6 to GA7.1 (Table 2) is explained by a single package change: Cld\_ON for LCA, Rad\_ON for CLI, and Mic\_ON for CLW. For LCA and CLW, most ON\_experiments

do not produce a substantial domain average change. For CLI, several ON\_experiments alter the GA6 domain average by more than  $\sim 10\%$ , including Cld\_ON and BL\_ON. These effects are, however, substantially less than the  $\sim 40\%$  change in Rad\_ON. Considering LCA, Cld\_ON overshoots the GA7.1 domain average but considering multiple package changes simultaneously (MicCldRad\_ON) the agreement with GA7.1 LCA is within  $\sim 0.5\%$ .

In contrast to cloud properties, multiple package changes are needed to explain the LW and SW CRE GA7.1-GA6 differences. The LW CRE differences between GA7.1 and GA6 (Table 2) is  $\sim 7\%$ . Most ON\_experiments do not produce a large change. Aer\_ON produces the greatest increase in LW CRE and most closely matches GA7.1 but is only 55% of the total GA7.1-GA6 difference. The largest absolute change is a decrease in LW CRE found in Cld\_ON, due to the reductions in LCA. Considering SW CRE, the overall GA7.1-GA6 difference is small resulting

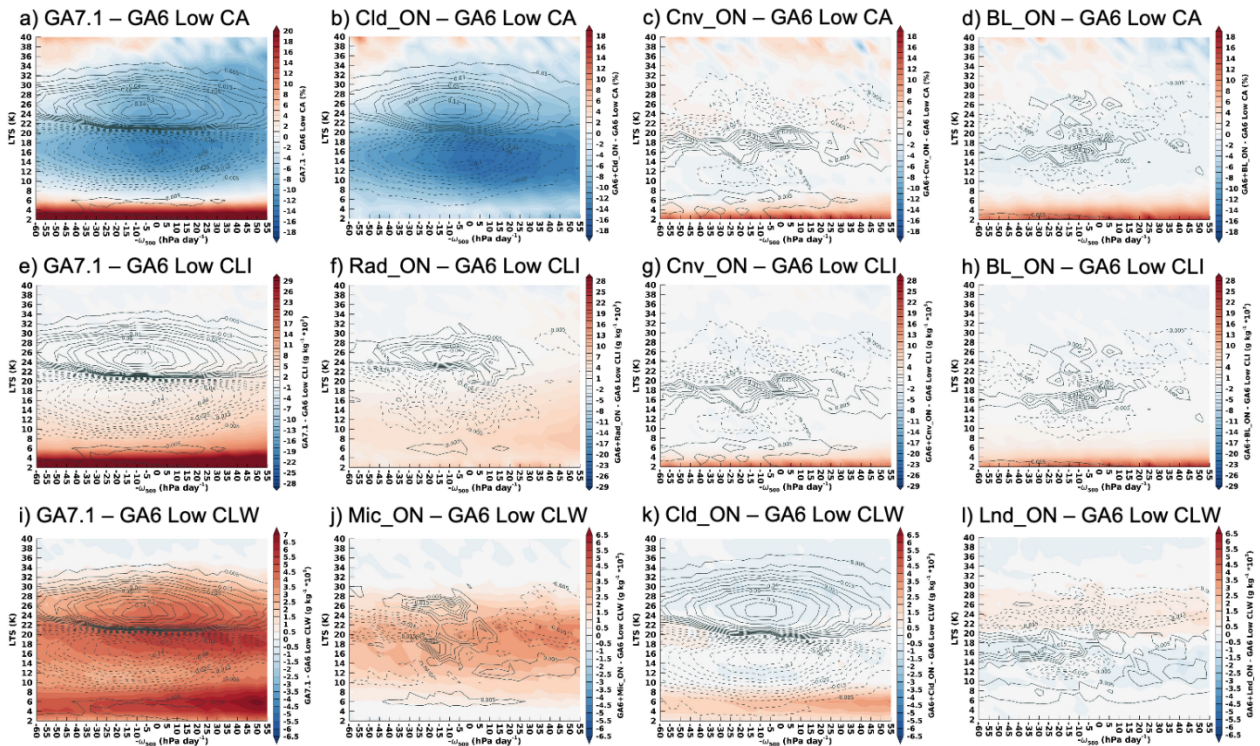


**Figure 5:** Annual mean differences between GA7.1 and GA6 and ON\_experiments and GA6 for (a-d) LCA, (e-h) CLI, and (i-l) CLW. Panels (a, e, i) GA7.1 minus GA6, (b, k) Cld\_ON minus GA6, (c, g) Cnv\_ON minus GA6, (d, h) BL\_ON minus GA6, (f) Rad\_ON minus GA6, (j) Mic\_ON minus GA6, and (l) Lnd\_ON minus GA6.

from offsetting effects of many parameterization changes.

As opposed to the domain average changes, multiple parameterization package changes are needed to explain the cloud property differences across meteorological regimes. Considering LCA, Fig. 5 shows that the Cld\_ON, Conv\_ON, and BL\_On experiments influence the distribution of GA7.1-GA6 cloud property changes across meteorological regimes. Cld\_ON (Fig. 5b) produces a general LCA decrease across most regimes; the Conv\_ON and BL\_ON experiments (Fig. 5c,d) are responsible for the LCA increase at LTS < 6 K. For CLI, Rad\_ON (Fig. 5f) produces the general CLI increase when LTS < 22 K and, as with LCA, Conv\_ON and BL\_ON experiments (Fig. 5g,h) are responsible for the CLI increase at LTS < 6 K. For CLW, Mic\_ON (Fig. 5j) produces the increase in CLW at LTS values between 10 and 28 K. Different from LCA and CLI, Cld\_ON (Fig. 5k) contains the increased CLW at LTS < 8 K, not Conv\_ON and BL\_ON.

Multiple parameterization packages are also needed to explain the LW and SW CRE changes across meteorological regimes. Interestingly, the MicCldRad\_ON experiment (Fig. 6b,g), which captures cloud property changes well, does not reproduce the LW and SW CRE GA7.1-GA6 differences in the domain average or in meteorological regimes. BL\_ON (Fig. 6c,h), Aer\_ON (Fig.

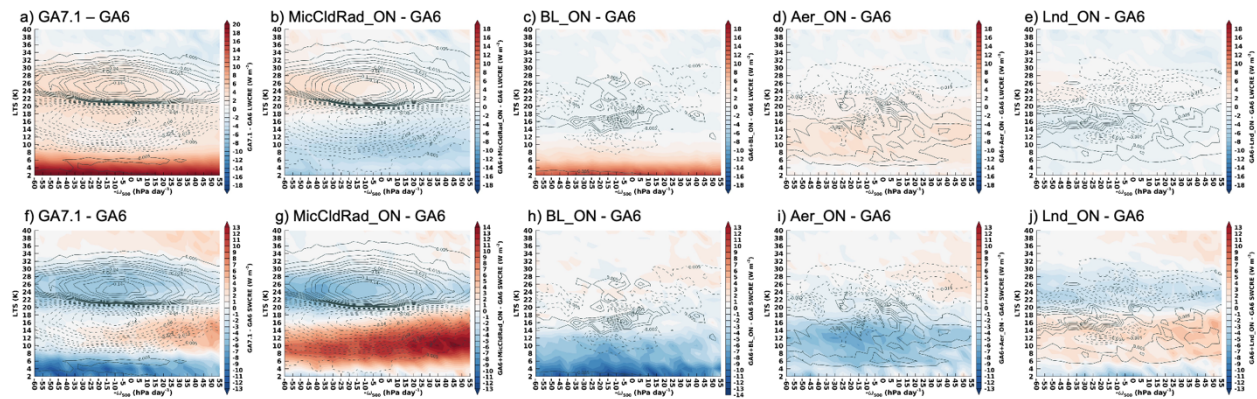


**Figure 6.** Annual mean differences between GA7.1 and GA6 and ON experiments and GA6 for (a-e) LW CRE and (f-j) SW CRE. Panels (a,f) GA7.1-GA6, (b,g) MicCldRad\_ON-GA6, (c,h) BL\_ON-GA6, (d,i) Aer\_ON-GA6, (e,j) Land\_ON-GA6. Units are  $W m^{-2}$ .

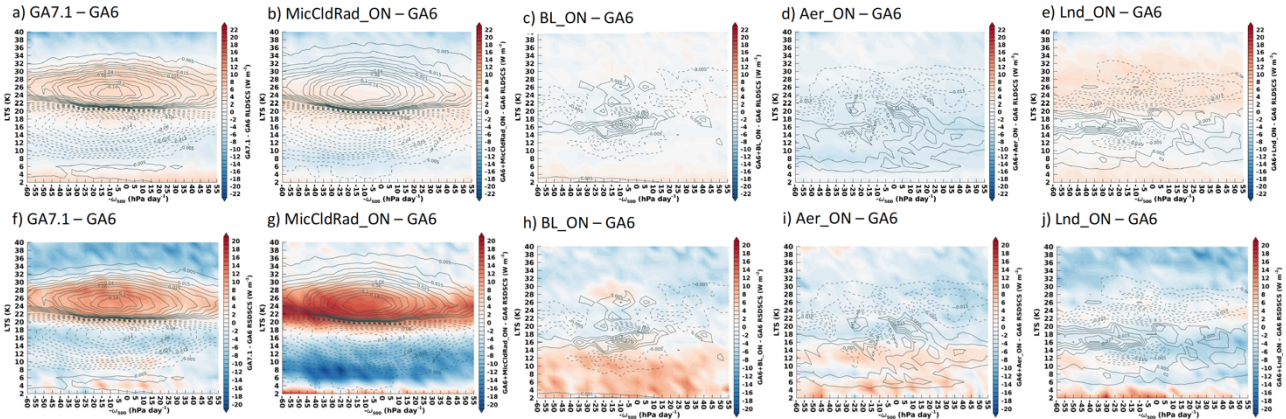


**Figure 7.** Annual mean differences in RLDSCS (a) GA7.1 - GA6, b) MicCldRad\_ON - GA6; c) BL\_ON - GA6; d) Aer\_ON - GA6 and e) Lnd\_ON - GA6. Figures (f) to (j): as (a) to (e) but for RSDSCS. Units are  $Wm^{-2}$ .

6d,i), and Lnd\_On (Fig. 6e,j) experiments also substantially influence the LW and SW CRE changes across meteorological regimes. This indicates that packages that do not influence cloud properties (referred to as “non-cloud” changes) influence the simulated LW and SW CRE.

We find that non-cloud parameterization packages substantially influence the GA7.1-GA6 LW and SW CRE differences by affecting the clear-sky fluxes. Considering RLDSCS, MicCldRad\_ON (Fig. 7b) and Lnd\_ON (Fig. 7e) exhibit a pattern that most closely resembles GA7.1-GA6 (Fig. 7a). In the available simulations, Lnd\_ON produces the largest positive change in RLDSCS. For RSDSCS (Fig. 7f-j), MicCldRad\_ON shows a strong influence on the RSDSCS with a similar pattern to GA7.1-GA6 (Fig. 7f) but stronger with a magnitude. Cloud parameterization changes contribute to substantial increases in RSDSCS for LTS from 20 to 28K and substantial decreases for LTS from 4-16 K. Several non-cloud scheme changes, including BL\_ON (Fig. 7h) and Aer\_On (Fig. 7i), offset these impacts on RSDSCS. The results indicate that the clear-sky flux response to cloud and non-cloud parameterization changes substantially influence LW and SW CRE.

Different ON\_experiments produce different RFO patterns, however Cld\_ON and Rad\_ON dominate the overall GA7.1-GA6 differences. The pattern shown by most ON\_experiments (Fig. 5) is a weak increase in the RFO for LTS from 14 to 22 K and a decrease in RFO at slightly larger

and smaller LTS with a weak  $-\omega_{500}$  dependence. Several parameterizations, specifically Mic\_ON (Fig. 5j) and Sto\_ON (not shown), show a RFO change with a greater dependence on  $-\omega_{500}$ . Most ON\_experiments show small RFO changes with a pattern that does not resemble GA7.1-GA6 differences (Fig. 5). Cld\_ON (Fig. 5b) and Rad\_ON (Fig. 5f) experiments show RFO change patterns that closely correspond to GA7.1-GA6. The RFO changes in the Rad\_ON experiment are  $\sim 25\%$  of the changes found in Cld\_ON. Thus, the Cld\_ON experiment provides the strongest influence on GA7.1-GA6 RFO changes. The results provide no evidence for a strong non-cloud parameterization influence on regime RFO changes.

Figure 8 shows a bar chart where the left most grouping represents the total cloud property change between GA7.1 (black bars) or an ON\_experiment (colored bars) and GA6. The remaining Fig. 8 groupings represent the regime independent, atmospheric regime dependent, and RFO terms, respectively. Considering LCA changes, the Cld\_ON experiment dominates the overall change; however, the regime independent term makes the largest contributions in Cld\_ON,

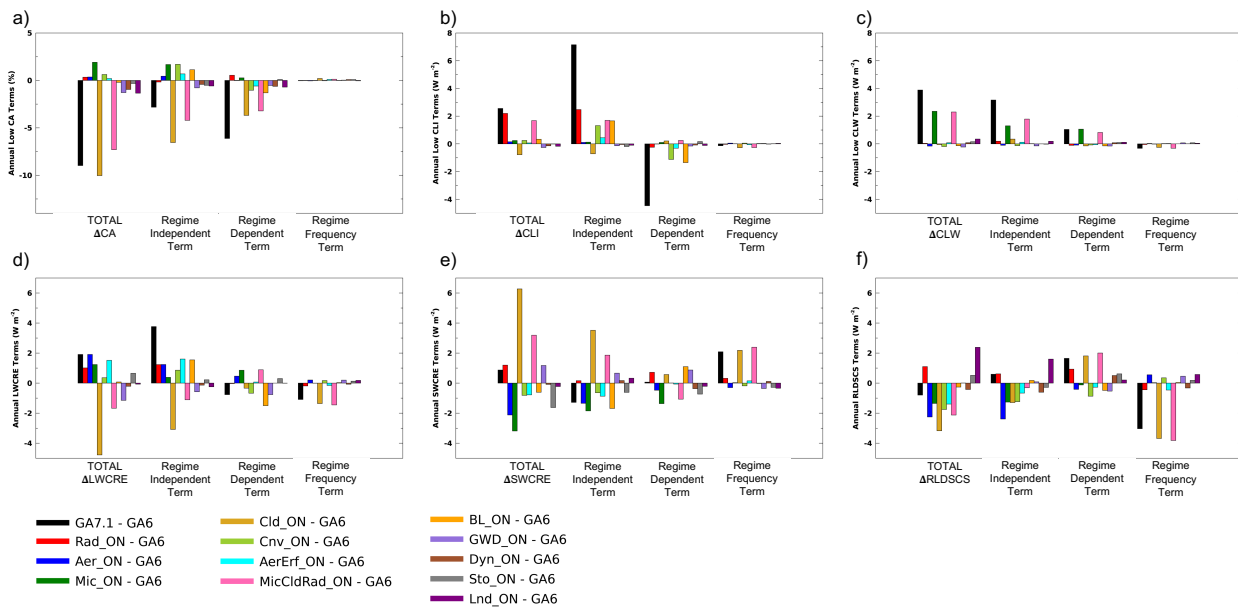


**Figure 8:** Contributions of the atmospheric-regime independent, atmospheric-regime dependent, and frequency of meteorological regime occurrence terms to the (a) LCA, (b) CLI, (c) CLW, (d) LW CRE, (e) SW CRE, and (f) RLDSCS to the annual mean GA7.1-GA6 and ON\_experiment-GA6 differences.

differing from Fig. 4 where the regime dependent term makes the largest contribution. Considering the CLI change, the overall contribution is dominated by Rad\_ON (as in Table 2). Rad\_ON, however, only influences the regime independent term while the GA7.1-GA6 change is from offsetting contributions of the regime independent and dependent terms. For CLW, Mic\_ON dominates the overall change and indicates little contribution from other experiments. The decomposition shows that other packages influence CLI but that their net contributions are small due to offsetting contributions from the regime independent and dependent terms. Since Rad\_ON does not produce a strong regime dependent contribution and the other ON\_experiments exhibit offsetting contributions, the source of the large negative contribution from the regime dependent term is unclear; parameterization interactions may explain this contribution.

For LW and SW CRE, many ON\_experiments contribute to the GA7.1-GA6 differences that provide contributions from all three decomposition terms. The Cld\_ON experiment shows offsetting contributions from the regime independent and RFO terms. This is interesting because the RFO change only has a substantial influence on the radiative flux terms and not the cloud property terms. As eluded to previously, the non-cloud parameterization experiments influence LW CRE by influencing the RLDSCS; Fig. 8 indicates that many parameterizations influence this flux. It is interesting that the primary way that the convection scheme influences LW CRE is through an influence on the RLDSCS flux. Lastly, while not making substantial contributions to the overall GA7.1-GA6 changes in any variable, the BL\_ON experiment shows offsetting contributions from the regime independent and dependent terms.

### 3.3. GA7.1 and GA6 differences from observations and reanalysis

This section compares GA7.1 and GA6 cloud properties with CERES SYN Ed4a and MERRA-2 to assess the alignment with observations. Comparisons are performed using average LCA, CLI,

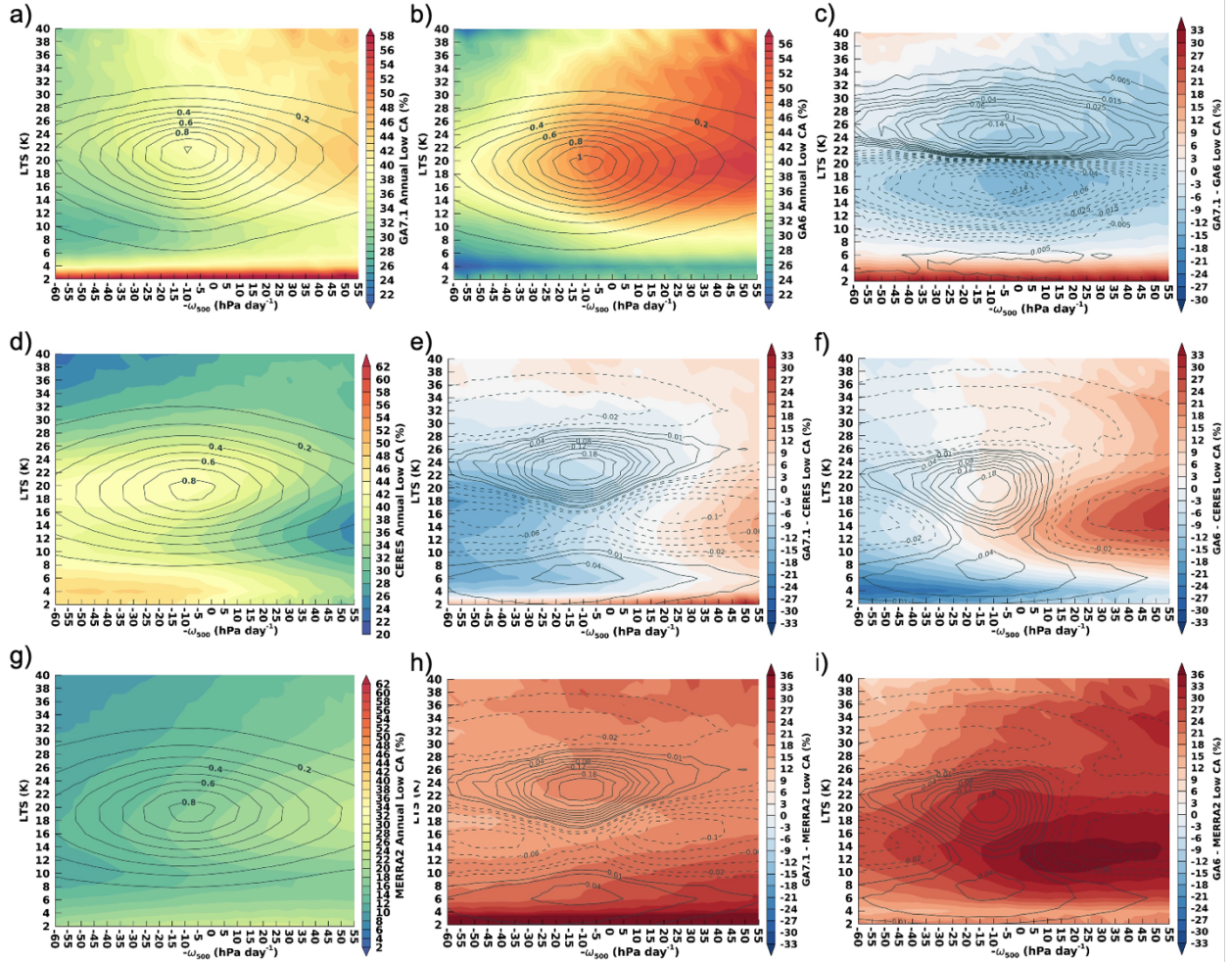


**Figure 9:** Annual mean LCA within LTS/ $-\omega_{500}$  meteorological regimes for (a) GA7.1, (b) GA6, (d) CERES, and (g) MERRA-2 and the (c) GA7.1-GA6, (e) GA7.1-CERES, (f) GA6-CERES, (h) GA7.1-MERRA-2, and (i) GA6-MERRA-2 differences.

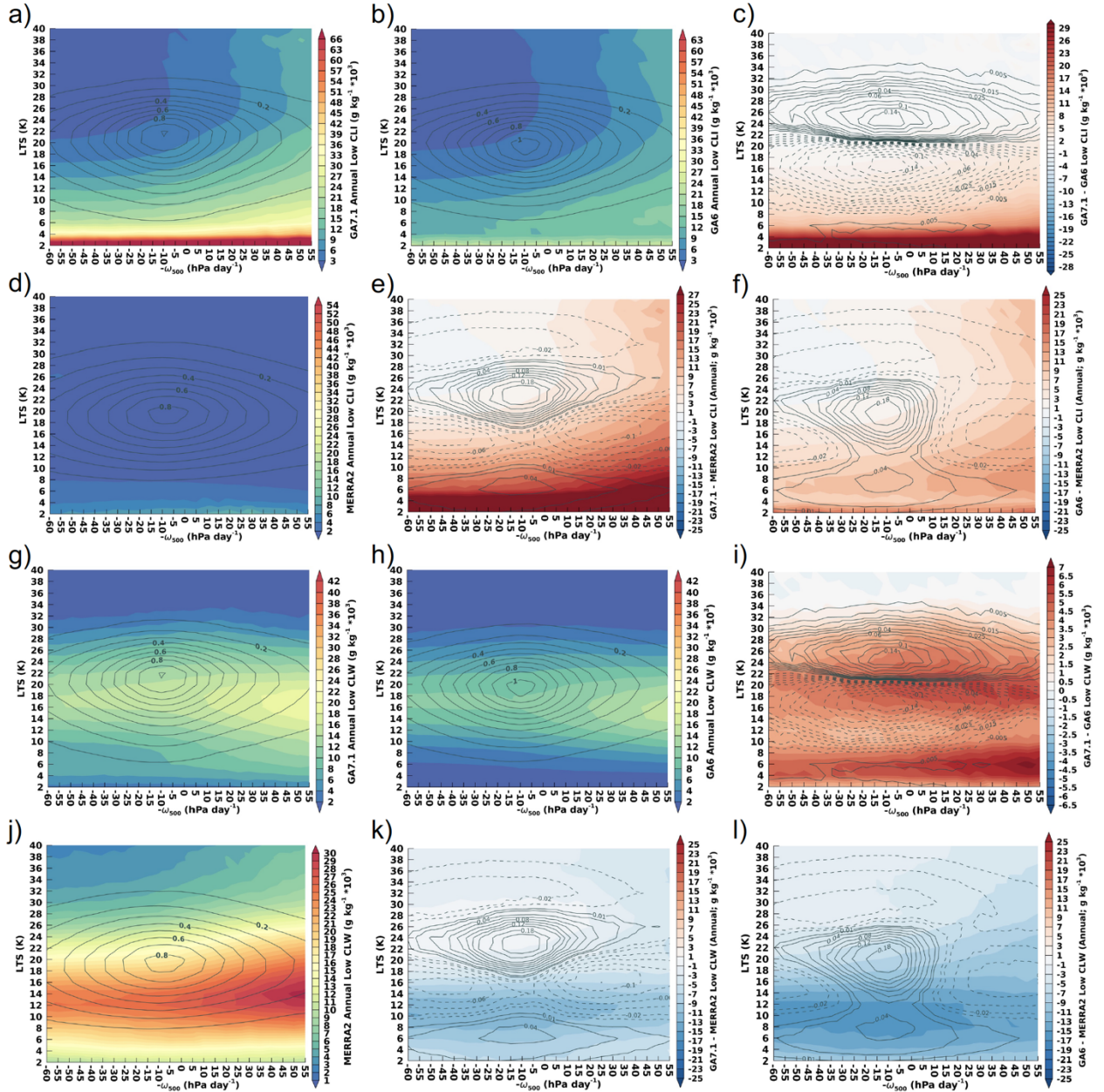
and CLW between the surface and 700 hPa for consistency with the CERES low cloud definition. Computing CRE using only downwelling all- and clear-sky fluxes reduces the impact of surface albedo differences between models and observations.

Figure 9 shows LCA across LTS/ $-\omega_{500}$  regimes for CERES, MERRA-2, and difference plots with GA6 and GA7.1. The LCA joint distributions for GA6, GA7.1 and MERRA-2 indicate increasing LCA for GA regimes with rising motion and medium-high stability (LTS  $\sim$  18 K) while CERES shows more clouds for subsidence regimes. The smaller LCA values for CERES clouds in regimes with rising motion result from passive satellite observations being blind to low clouds

under high clouds. Spaceborne radar measurements show that low clouds are found in these regimes (e.g., Taylor et al. 2015; Yu et al. 2019). Performing this comparison using satellite simulator output is a better method (e.g., Bodas-Salcedo et al. 2011; Kay et al. 2012; Medeiros et al. 2023), however satellite simulator output is not available for these simulations. While MERRA-2 possesses shortcomings in its representation of Arctic low clouds producing too few clouds (Segal Rozenhaimer et al. 2018); the differences between GA7.1 and GA6 with MERRA-2 are the most appropriate comparison for assessing alignment with the observed Arctic clouds. All reanalysis products exhibit shortcomings in the Arctic (Yeo et al. 2022); MERRA-2 is used here as it provides a reasonable representation of the general Arctic cloud properties.

GA6 and GA7.1 LCA compare similarly with MERRA-2 showing the largest differences under rising motion and lower LTS values. The GA7.1 and GA6 also show RFO differences with MERRA-2 (Table 2); however, these differences have a small influence. While GA6 and GA7.1 simulate less LCA than found in MERRA-2, Fig. 9 indicates that GA7.1 is in better overall agreement with MERRA-2.

GA6 and GA7.1 both simulate greater CLI and less CLW than MERRA-2. Figure 10 shows joint distributions for CLI and CLW from reanalysis and differences with GA6 and GA7.1. The greatest CLI for both models and MERRA-2 is found in low stability regimes ( $LTS < 4K$ ), though magnitudes vary greatly. Outside of these low stability regimes, model simulations show a similar dependence of CLI and similar differences with MERRA-2. The GA7.1 and GA6 differences with MERRA-2 are generally regime independent. While the differences between GA7.1 and GA6 with MERRA-2 are substantial, the results suggest that GA6 CLI agrees better with MERRA-2 and GA7.1 shows better agreement with MERRA-2 for CLW.



**Figure 10.** Annual mean (a-f) CLI and (g-l) CLW within LTS/ $-\omega_{500}$  meteorological regimes for (a,g) GA7.1, (b,h) GA6, and (d,j) MERRA-2 and the (c,i) GA7.1-GA6, (e,k) GA7.1-MERRA-2, and (f,l) GA6-MERRA-2 differences. Units are in  $10^{-3} \text{ g kg}^{-1}$

Figure 11 shows the joint distributions of observed and modeled LW CRE (Fig 11a-f) and SW CRE (Fig 11g-l). Maximum LW CRE occurs at  $\sim \text{LTS} < 20 \text{ K}$  for both CERES and models and increases with decreasing stability, though both GA6 and GA7.1 show a dependence on  $-\omega_{500}$  that is not found in observations. CERES LW CRE is larger than GA6 and GA7.1 for mid-high stability

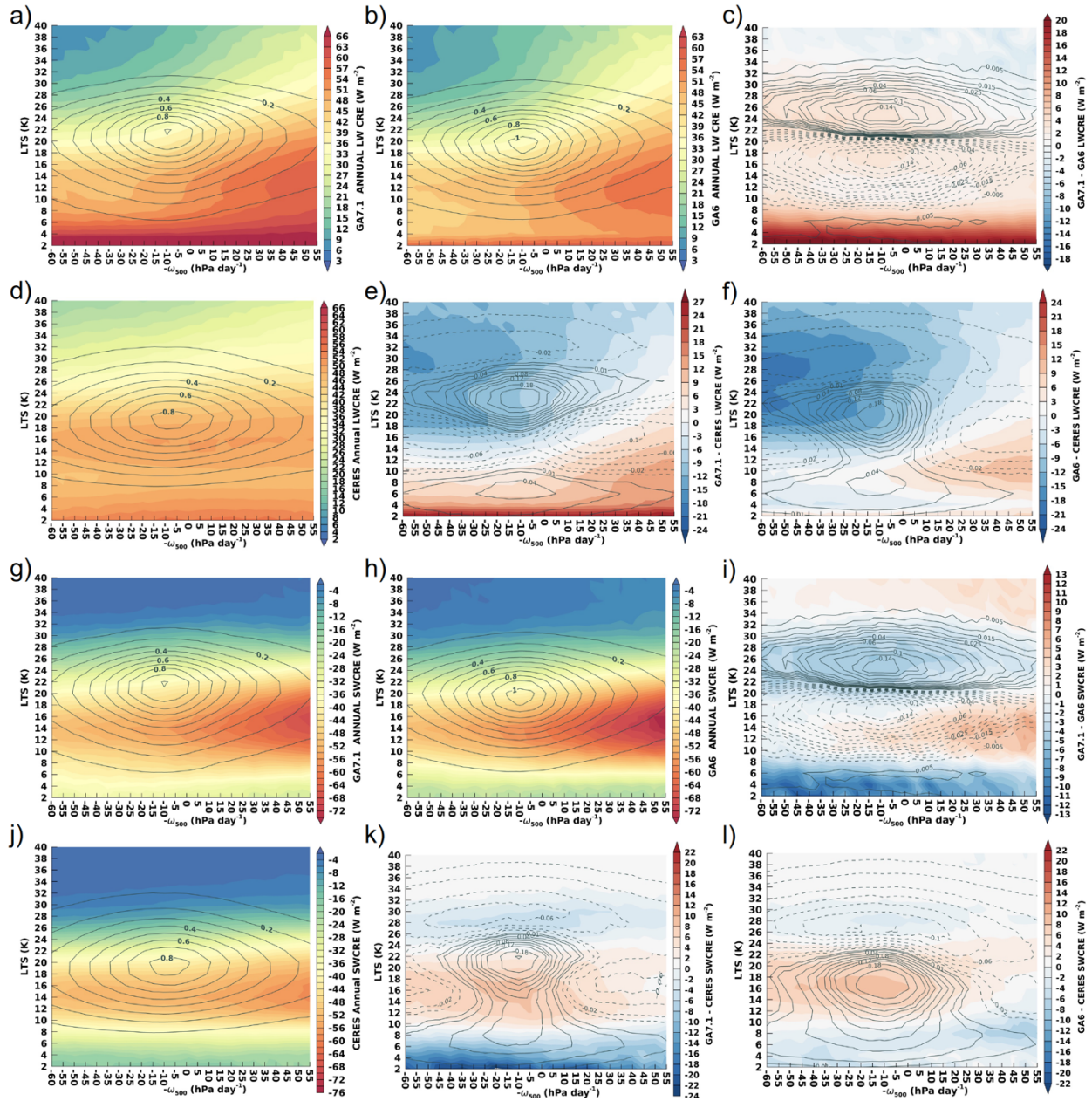


**Figure 11.** Annual mean (a-f) LW and (g-l) SW CRE within LTS/ $-\omega_{500}$  meteorological regimes for (a,g) GA7.1, (b,h) GA6, and (d, j) CERES and the (c, i) GA7.1-GA6, (e,k) GA7.1-CERES, and (f,l) GA6-CERES differences. Units are in  $\text{Wm}^{-2}$ .

regimes, particularly with increasing subsidence. Negative LW CRE differences occur in regimes more frequently simulated by models and contribute to the lower model mean LW CRE. Both GA7.1 and GA6 simulate low stability regimes more frequently than MERRA-2, which for GA7.1 contain mostly positive LW CRE differences ( $\text{GA7.1} > \text{CERES}$ ) while for GA6 these regimes have smaller, slightly negative LW CRE differences ( $\text{CERES} > \text{GA6}$ ). The largest model

differences in LW CRE (Fig. 11c) occur for low stability regimes coinciding with the large inter-model differences in ice clouds present at  $LTS < 4$  K, indicating that changes in CLI are driving radiative differences in GA7.1 farther from CERES observations.

Considering SW CRE (Figure 11g-l), maximum SW CRE for GA6, GA7.1 and CERES is found for rising motion and medium stability with minimum SW CRE found in high stability regimes independent of  $-\omega_{500}$ . These regimes are more frequently simulated in GA7.1 than GA6 (solid line contours in Fig. 11i) and possess larger SW CRE, larger LW CRE, about the same CLI, more CLW, and smaller LCA for GA7.1 compared to GA6. These more frequently simulated regimes do not coincide with the largest inter-model differences and, in the case of LCA, are not coincident with the sign of the largest inter-model differences. If the frequency of low stability regimes increases—either through model improvement or from climate change—larger inter-model biases may be seen.

The takeaway from this comparison is that overall GA7.1 shows better agreement with observations than GA6. However, this is not the case under all conditions. The most notable regimes under which GA6 outperforms GA7.1 are those with low LTS conditions. Overall, GA6 and GA7.1 cloud properties tend to be more like each other than like MERRA-2.

#### 4. Discussion

The conventional approach for improving model-simulated cloud properties and their radiative effects revolves around using (new) in situ or satellite observations to guide the refinement of an existing cloud parameterization or development of a new one (e.g., Field et al. 2007; Molod 2012; Morcrette 2012; Bouttle and Abel 2012; Bouttle et al. 2014; Barahona et al. 2014; Molod et al. 2015). At the heart of this conventional approach is a cloud parameterization. However, a key finding of this paper is the influence of non-cloud parameterizations on LW and SW CRE through

their impact on clear-sky fluxes. The importance of clear-sky fluxes to CRE is evident the definition of CRE and has been discussed in many previous studies (e.g., Sohn et al. 2006; Soden et al. 2008; Boeke and Taylor 2016; Loeb et al. 2020). The influence of cloud parameterization on model-simulated CRE is clear and we document the substantial contributions of non-cloud parameterizations. To the best of our knowledge the contributions of non-cloud parameterizations to model-simulated CRE have not been documented. Thus, non-cloud parameterizations must be considered to understand the full influence of parameterization changes on CRE.

Cloud parameterizations are also found to influence clear-sky fluxes and do so differently by meteorological regime. The influence of cloud parameterizations on clear-sky fluxes indicates a potential feedback/interaction between the cloud properties, the atmospheric circulation, and the clear-sky fluxes that requires further exploration to understand. This effect differs from the influence of different definitions of clear-sky fluxes on CRE.

Many studies highlight the importance of two-way interactions between clouds and the atmospheric circulation (e.g., Li et al. 2015; Ceppi and Hartman 2016; Voigt et al. 2021). We find that the large-scale cloud scheme is the single most impactful parameterization on the changes in the frequency of Arctic meteorological regimes between GA6 and GA7.1. It is known that the large-scale atmospheric circulation responds to the influence of clouds on the atmospheric heating rate profile. Assuming that the cloud influence on the atmospheric heating rate profile is determined to first order by the presence or absence of clouds, it follows that the parameterization that dictates cloud amount would strongly impact the regime RFO. It is not clear, however, why other parameterizations do not more strongly influence the RFO. This result suggests, at least for this model, that cloud presence plays the most important role in determining the meteorological regime occurrence. Thus, this effect could represent an important interaction between clouds and

regime occurrence that enables other mechanisms to influence the atmospheric circulation by impacting cloud amount. For instance, a response of clouds to sea ice loss (e.g., Kay and Gettelman 2009; Taylor et al. 2015; Morrison et al. 2018) could alter the cloud amount and modulate the atmospheric circulation. There is has been much debate over the influence of sea ice loss on the Arctic-mid latitude circulation (e.g., Cohen et al. 2020) and Arctic Amplification (Hahn et al. 2021; Taylor et al. 2022; Tan et al. 2023) and this result suggests that a portion of the uncertainty could be related to the cloud response to sea ice.

The present study informs observations in two important ways. First, the RFO distribution indicates the specific atmospheric conditions that make the largest contributions to the mean model-simulated cloud properties and radiative effects. Thus, targeted observation campaigns gathering cloud properties and process data within these most frequently occurring regimes will provide the most value for improving the mean model-simulated cloud properties.

Secondly, the analysis identifies atmospheric conditions with the largest differences between the models and observations; regimes of the greatest differences should also be targeted. Weak LTS regimes and strong LTS regimes under subsidence show the largest difference. This provokes an interesting notion and question. Could cloud properties within infrequently occurring regimes have a strong influence on the atmospheric circulation and the model-simulated response to climate change? Weak LTS regimes and strong LTS regimes under subsidence occur infrequently and, thus, do not significantly contribute to the domain-averaged differences between the models or with observations. Is there value in chasing observations of these infrequently occurring regimes? It is an open question as to whether the most frequently occurring regimes, the regimes with the largest sensitivity, or other regimes are most important to the climate change simulations.

It is clear that the meteorological regime approach exposes regime differences between the models and observations that go undetected when using top-level diagnostics. This information can be useful information for developers to better understand model behavior and the influence of parameterization changes. The sensitivity of climate simulations to the representation of clouds under specific meteorological conditions has not been systematically explored and the importance of accurate modeling of clouds under infrequently occurring conditions is unclear. A meteorological regime specific cloud-locking experiment may provide insight into this question.

## 5. Conclusion

In closing, this paper explores the contributions of individual parameterization package updates to changes in Arctic low cloud properties between the two versions of the HadGEM3 atmospheric model (GA6 and GA7.1) using a suite of model experiments. We find that the effect of changing a parameterization depends upon the meteorological regime and that there are often compensating changes between regimes. However, the largest changes in cloud properties can be attributed to single individual parameterizations schemes: low cloud amount to the large-scale cloud scheme, cloud liquid water to the cloud microphysics scheme, and cloud ice concentration to the radiation scheme. Multiple parameterizations contribute to differences in LW and SW CRE between model versions with a substantial contribution from changes in clear-sky fluxes from both the cloud and non-cloud parameterization changes. The results indicate that the parameterization changes have different influences on the meteorological regime independent, regime dependent, and regime frequency change contributions to the cloud property differences.

We conclude that the regime decomposition approach, showing contributions from different meteorological regimes, is useful for model evaluation against observations and when trying to understand changes between model versions and when assessing the regimes that should be

targeted by observations. The regime approach highlights that domain averaged changes in cloud properties due to parameterization changes or under climate change can strongly depend upon the meteorological regime. The results indicate that processes that do not directly influence the cloud properties but influence the regime frequency of occurrence and/or the regime thermodynamic properties are also found to influence the domain average cloud properties and model biases. Lastly, the regime decomposition approach provides a more complete view of the model-simulated cloud response to a parameterization change highlighting the impacts of a parameterization change under conditions that are do not frequently occur and are often overlooked or missed by conventional model diagnostics.

### ***Acknowledgements***

PCT and RCB are supported by the NASA Interdisciplinary Studies Program Grant 80NSSC21K0264 and the NASA Radiation Budget Science Project. ABS was supported by the Met Office Hadley Centre Climate Programme funded by DSIT.

### **Open Research**

*Data Availability Statement:* CERES SYN Ed4a radiative fluxes and cloud properties data (NASA/LARC/SD/ASDC; 2017) are freely available and can be accessed at [asdc.larc.nasa.gov](https://asdc.larc.nasa.gov). MERRA-2 (GMAO 2015) data are available at the GES DISC (<https://disc.gsfc.nasa.gov/datasets?project=MERRA-2>).

## 6. References

- Alkama, R., Cescatti, A., Taylor, P. C., Garcia-San Martin, L., Douville, H., Duveiller, G., et al. (2020). Clouds damp the radiative impacts of polar sea ice loss. *The Cryosphere*, 14, 2673–2686. <https://doi.org/10.5194/tc-14-2673-2020>
- Barahona, D., Molod, A., Bacmeister, J., Nenes, A., Gettelman, A., Morrison, H., Phillips, V., and Eichmann, A. (2014), Development of two-moment cloud microphysics for liquid and ice within the NASA Goddard Earth Observing System Model (GEOS-5), *Geosci. Model Dev.*, 7, 1733–1766, <https://doi.org/10.5194/gmd-7-1733-2014>.
- Baran, A. J., Hill, P., Walters, D., Hardman, S. C., Furtado, K., Field, P. R., and Manners, J., 2016: The impact of two coupled cirrus microphysics-radiation parameterizations on the temperature and specific humidity biases in the tropical tropopause layer in a climate model, *J. Climate*, 29, 5299–5316, <https://doi.org/10.1175/JCLI-D-15-0821.1>.
- Barton, N. P., Klein, S. A., Boyle, J. S., & Zhang, Y. Y. (2012). Arctic synoptic regimes: Comparing domain-wide Arctic cloud observations with CAM4 and CAM5 during similar dynamics. *Journal of Geophysical Research*, 117, D15205. <https://doi.org/10.1029/2012JD017589>
- Bodas-Salcedo, A., and Coauthors, 2011: COSP: Satellite simulation software for model assessment. *Bull. Amer. Meteor. Soc.*, 92, 1023–1043, <https://doi.org/10.1175/2011BAMS2856.1>.
- Bodas-Salcedo, A., Mulcahy, J. P., Andrews, T., et al. (2019). Strong dependence of atmospheric feedbacks on mixed-phase microphysics and aerosol-cloud interactions in HadGEM3. *Journal of Advances in Modeling Earth Systems*, 11, 1735–1758. <https://doi.org/10.1029/2019MS001688>.
- Boeke, R. C. and P. C. Taylor (2016), Evaluation of the Arctic surface radiation budget in CMIP5 models. *J. Geophys. Res.*, **121**, 8525–8548, doi: 10.1002/2016JD025099.
- Boeke, R. C. and Taylor, P. C. (2018). Seasonal energy exchange in sea ice retreat regions contributes to differences in projected Arctic warming. *Nature Communications* **9**, 5017.
- Boutle, I. A. and Abel, S. J. (2012), Microphysical controls on the stratocumulus topped boundary-layer structure during VOCALS-REx, *Atmos. Chem. Phys.*, 12, 2849–2863, <https://doi.org/10.5194/acp-12-2849-2012>, 2012.
- Boutle, I. A., Abel, S. J., Hill, P. G., and Morcrette, C. J. (2014), Spatial variability of liquid cloud and rain: observations and microphysical effects, *Q. J. Roy. Meteorol. Soc.*, 140, 583–594, <https://doi.org/10.1002/qj.2140>.
- Ceppi, P., and P. Nowack (2021). Observational evidence that cloud feedback amplifies global warming. *Proceed. Natl. Acad. Sci.*, **118**(30) e2026290118, doi: <http://doi.org/10.1073/pnas.2026290118>.

Chylek, P., Folland, C., Klett, J. D., Wang, M., Hengartner, N., Lesins, G., & Dubey, M. K. (2022). Annual mean Arctic Amplification 1970–2020: Observed and simulated by CMIP6 climate models. *Geophysical Research Letters*, 49, e2022GL099371. <https://doi.org/10.1029/2022GL099371>

Cohen, J. and coauthors (2020), Divergent consensus on Arctic amplification influence on midlatitude severe winter weather. *Nat. Clim. Chang.* **10**, 20–29, <https://doi.org/10.1038/s41558-019-0662-y>.

Cotton, R. J., Field, P. R., Ulanowski, Z., Kaye, P. H., Hirst, E., Greenaway, R. S., Crawford, I., Crosier, J., and Dorsey, J. (2013), The effective density of small ice particles obtained from in situ aircraft observations of mid-latitude cirrus, *Q. J. Roy. Meteorol. Soc.*, 139, 1923–1934, <https://doi.org/10.1002/qj.2058>.

Curry, J. A., Schramm, J. L., Rossow, W. B., & Randall, D. (1996). Overview of Arctic cloud and radiation characteristics. *Journal of Climate*, 9(8), 1731–1764. [https://doi.org/10.1175/1520-0442\(1996\)009<1731:OOACAR>2.0.CO;2](https://doi.org/10.1175/1520-0442(1996)009<1731:OOACAR>2.0.CO;2)

Doelling, D. R., N. G. Loeb, D. F. Keyes, M. L. Nordeen, D. Morstad, C. Nguyen, B. A. Wielicki, D. F. Young, and M. Sun (2013), Geostationary enhanced temporal interpolation for CERES flux products, *J. Atmos. Oceanic Technol.*, 30, 1072–1090, doi:10.1175/JTECH-D-12-00136.1.

Doelling, D. R., M. Sun, L. T. Nguyen, M. L. Nordeen, C. O. Haney, D. F. Keyes, P. E. Mlynchak (2016), Advances in Geostationary-Derived Longwave Fluxes for the CERES Synoptic (SYN1deg) Product, *J. Atmos. Ocean. Techn.*, **33**(3), 503–521. doi: 10.1175/JTECH-D-15-0147.1

Donohoe, A., Blanchard-Wrigglesworth, E., Schweiger, A., and Rasch, P. J. (2020). The Effect of Atmospheric Transmissivity on Model and Observational Estimates of the Sea Ice Albedo Feedback. *J. Clim.* 33 (13), 5743–5765. doi:10.1175/JCLI-D-19-0674.1

Edwards, J. M. and Slingo, A. (1996), Studies with a flexible new radiation code. I: Choosing a configuration for a large-scale model, *Q. J. Roy. Meteorol. Soc.*, 122, 689–719, <https://doi.org/10.1002/qj.49712253107>.

English, J. M., J. E. Kay, A. Gettelman, X. Liu, Y. Wang, Y. Zhang, and H. Chepfer (2014), Contributions of clouds, surface albedo, and mixed-phase ice nucleation schemes to Arctic radiation biases in CAM5. *J. Climate*, **27**, 5174–5197, doi:10.1175/JCLI-D-13-00608.1.

Field, P. R., Heymsfield, A. J., and Bansemer, A. (2007), Snow Size Distribution Parameterization for Midlatitude and Tropical Ice Clouds, *J. Atmos. Sci.*, 64, 4346–4365, <https://doi.org/10.1175/2007JAS2344.1>, 2007.

Field, P. R., Hill, A. A., Furtado, K., and Korolev, A. (2014), Mixed-phase clouds in a turbulent environment. Part 2: Analytic treatment, *Q. J. Roy. Meteorol. Soc.*, 140, 870–880, <https://doi.org/10.1002/qj.2175>.

Furtado, K., Field, P. R., Boutle, I. A., Morcrette, C. J., and Wilkinson, J. M. (2016), A physically based subgrid parameterization for the production and maintenance of mixed-phase clouds in a general circulation model, *J. Atmos. Sci.*, **73**, 279–291, <https://doi.org/10.1175/JAS-D-15-0021.1>.

Gelaro, R., and coauthors (2017), The Modern-Era Retrospective Analysis for Research and Applications, Version 2 (MERRA-2). *J. Climate*, **30**, 5419-5454, <https://doi.org/10.1175/JCLI-D-16-0758.1>.

Gettelman, A., X. Liu, S. J. Ghan, H. Morrison, S. Park, A. J. Conley, S. A. Klein, J. Boyle, D. L. Mitchell, and J.-L. F. Li (2010), Global simulations of ice nucleation and ice supersaturation with an improved cloud scheme in the Community Atmosphere Model, *J. Geophys. Res.*, **115**, D18216, doi:10.1029/2009JD013797.

Global Modeling and Assimilation Office (GMAO) (2015), *tavg1\_2d\_rad\_Nx: MERRA-2 3D IAU State, Meteorology Instantaneous 1-hourly (p-coord, 0.625x0.5L42), version 5.12.4*, Greenbelt, MD, USA: Goddard Space Flight Center Distributed Active Archive Center, Last accessed 3/23/2023 at doi:10.5067/Q9QMY5PBNV1T.

Hahn L.C., Armour K.C., Zelinka M.D., Bitz C.M. and Donohoe A. (2021), Contributions to Polar Amplification in CMIP5 and CMIP6 Models. *Front. Earth Sci.* **9**:710036. doi: 10.3389/feart.2021.710036

Hill, P. G., Morcrette, C. J., and Boutle, I. A. (2015), A regime-dependent parametrization of subgrid-scale cloud water content variability, *Q. J. Roy. Meteorol. Soc.*, **141**, 1975–1986, <https://doi.org/10.1002/qj.2506>.

Huang, Y. P. C. Taylor, D. Rutan, F. Rose, M. Shupe (2022), Toward a more realistic representation of surface albedo in NASA CERES-derived surface radiative fluxes: A comparison with MOSAIC field campaign, *Elem. Sci. Anth.*, **10**:1, <https://doi.org/10.1515/elementa.2022.00013>.

Jianfen Wei, Zhaomin Wang, Mingyi Gu, Jing-Jia Luo, Yunhe Wang. An evaluation of the Arctic clouds and surface radiative fluxes in CMIP6 models[J]. *Acta Oceanologica Sinica*, 2021, 40(1): 85-102. doi: [10.1007/s13131-021-1705-6](https://doi.org/10.1007/s13131-021-1705-6)

Kato, S., Sun-Mack, S., Miller, W. F., Rose, F. G., Chen, Y., Minnis, P., & Wielicki, B. A. (2010). Relationships among cloud occurrence frequency, overlap, and effective thickness derived from CALIPSO and CloudSat merged cloud vertical profiles, *Journal of Geophysical Research*, **115**, D00H28, doi:10.1029/2009JD012277.

Kato, S., Rose, F. G., Sun-Mack, S., Miller, W. F., Chen, Y., Rutan, D. A., et al. (2011). Improvements of top-of-atmosphere and surface irradiance computations with CALIPSO-, CloudSat-, and MODIS-derived cloud and aerosol properties. *Journal of Geophysical Research*, **116**, D19209. <https://doi.org/10.1029/2011JD016050>

- Kay, J. E., and Gettelman, A. (2009). Cloud influence on and response to seasonal Arctic sea ice loss. *Journal of Geophysical Research*, 114, D18204. <https://doi.org/10.1029/2009JD011773>
- Kay, J. E., and coauthors (2012), Exposing global cloud biases in the community atmosphere model (CAM) using satellite observations and their corresponding instrument simulators. *J. Climate*, **25**, 5190-5207. <https://doi.org/10.1175/JCLI-D-11-00469.1>.
- Klaus, D., K. Dethloff, W. Dorn, A. Rinke, and D. L. Wu (2016), New insight of Arctic cloud parameterization from regional climate model simulations, satellite-based, and drifting station data, *Geophys. Res. Lett.*, 43, 5450–5459, doi:[10.1002/2015GL067530](https://doi.org/10.1002/2015GL067530).
- Komurcu, M., T. Storelvmo, I. Tan, U. Lohmann, Y. Yun, J. E. Penner, Y. Wang, X. Liu, and T. Takemura (2014), Intercomparison of the cloud water phase among global climate models, *J. Geophys. Res. Atmos.*, 119, 3372–3400, doi:[10.1002/2013JD021119](https://doi.org/10.1002/2013JD021119).
- Li, Y. D. W. J. Thompson and S. Bony (2015), The influence of atmospheric cloud radiative effects on the large-scale atmospheric circulation. *J. Climate*, **28**, 7263-7278, <https://doi.org/10.1175/JCLI-D-14-00825.1>.
- Liu, Z. and Schweiger, A. (2017). Synoptic Conditions, Clouds, and Sea Ice Melt Onset in the Beaufort and Chukchi Seasonal Ice Zone, *Journal of Climate*, 30(17), 6999-7016. Retrieved May 24, 2022, from <https://journals.ametsoc.org/view/journals/clim/30/17/jcli-d-16-0887.1.xml>
- Loeb, N. G., and coauthors (2020), Toward a consistent definition between satellite and model clear-sky radiative fluxes. *J. Climate*, **33**, 61-75, <https://doi.org/10.1175/JCLI-D-19-0381.1>.
- Manners, J., Edwards, J. M., Hill, P., and Thelen, J.-C. (2015), SOCRATES (Suite Of Community Radiative Transfer codes based on Edwards and Slingo) Technical Guide, Met Office, UK, available at: <https://code.metoffice.gov.uk/trac/socrates> (last access: 12 October 2023).
- McGraw, Z., Storelvmo, T., Polvani, L. M., Hofer, S., Shaw, J. K., & Gettelman, A. (2023). On the links between ice nucleation, cloud phase, and climate sensitivity in CESM2. *Geophysical Research Letters*, 50, e2023GL105053. <https://doi.org/10.1029/2023GL105053>
- Medeiros, B., Shaw, J., Kay, J. E., & Davis, I. (2023). Assessing clouds using satellite observations through three generations of global atmosphere models. *Earth and Space Science*, 10, e2023EA002918. <https://doi.org/10.1029/2023EA002918>.
- Molod, A. (2012), Constraints on the profile of total water PDF in AGCMs from AIRS and a high-resolution model. *J. Climate*, **25**, 8341-8352, <https://doi.org/10.1175/JCLI-D-11-00412.1>.
- Molod, A., Takacs, L., Suarez, M., and Bacmeister, J. (2015), Development of the GEOS-5 atmospheric general circulation model: evolution from MERRA to MERRA2, *Geosci. Model Dev.*, 8, 1339–1356, <https://doi.org/10.5194/gmd-8-1339-2015>.

- Morcrette, C.J. (2012), Improvements to a prognostic cloud scheme through changes to its cloud erosion parametrization. *Atmosph. Sci. Lett.*, **13**, 95-102. <https://doi.org/10.1002/asl.374>
- Morrison, H., G. de Boer, G. Feingold, J. Harrington, M. D. Shupe, and K. Sulia (2012), Resilience of persistent Arctic mixed-phase clouds, *Nat. Geosci.*, **5**, 11–17, doi:10.1038/ngeo1332.
- Morrison, A. L., Kay, J. E., Chepfer, H., Guzman, R., & Yettella, V. (2018). Isolating the liquid cloud response to recent Arctic sea ice variability using spaceborne lidar observations. *Journal of Geophysical Research: Atmospheres*, **123**, 473–490. <https://doi.org/10.1002/2017JD027248>
- Mulcahy, J. P., Jones, C., Sellar, A., et al. (2018), Improved aerosol processes and effective radiative forcing in HadGEM3 and UKESM1. *Journal of Advances in Modeling Earth Systems*, **10**, 2786–2805. <https://doi.org/10.1029/2018MS001464>.
- NASA/LARC/SD/ASDC (2017). CERES and GEO-enhanced TOA, within-atmosphere and surface fluxes, clouds and aerosols 1-hourly terra-aqua Edition4A. NASA Langley Atmospheric Science Data Center DAAC. [https://asdc.larc.nasa.gov/project/CERES/CER\\_SYN1deg-1Hour\\_Terra-Aqua-MODIS\\_Edition4](https://asdc.larc.nasa.gov/project/CERES/CER_SYN1deg-1Hour_Terra-Aqua-MODIS_Edition4).
- Pithan, F., Medeiros, B. & Mauritsen, T. (2014), Mixed-phase clouds cause climate model biases in Arctic wintertime temperature inversions. *Clim Dyn* **43**, 289–303. <https://doi.org/10.1007/s00382-013-1964-9>.
- Previdi, M., K. L. Smith, L. M. Polvani (2021). Arctic amplification of climate change: A review of underlying mechanisms. *Environ. Res. Lett.*, **16**, 093003, doi: 10.1017/1748-9326/ac1c29.
- Rantanen, M., Karpechko, A.Y., Lipponen, A. *et al.* (2022). The Arctic has warmed nearly four times faster than the globe since 1979. *Commun Earth Environ.*, **3**, 168. <https://doi.org/10.1038/s43247-022-00498-3>
- Rutan, DA, Kato, S, Doelling, DR, Rose, FG, Nguyen, LT, Caldwell, TE, Loeb, NG. 2015. CERES synoptic product: Methodology and validation of surface radiant flux. *Journal of Atmospheric and Oceanic Technology* **32**(6): 1121-1143.
- Segal Rozenhaimer, M., Barton, N., Redemann, J., Schmidt, S., LeBlanc, S., Anderson, B., et al. (2018). Bias and sensitivity of boundary layer clouds and surface radiative fluxes in MERRA-2 and airborne observations over the Beaufort Sea during the ARISE campaign. *Journal of Geophysical Research: Atmospheres*, **123**, 6565–6580. <https://doi.org/10.1029/2018JD028349>
- Sledd, A., and L'Ecuyer, T. S. (2021). Emerging trends in Arctic solar absorption. *Geophysical Research Letters*, **48**, e2021GL095813. <https://doi.org/10.1029/2021GL095813>.
- Sledd, A., L'Ecuyer, T. (2019). How much do clouds mask the impacts of Arctic sea ice and snow cover variations? Different perspectives from observations and reanalyses. *Atmosphere*, **10**(1),12. <https://doi.org/10.3390/atmos10010012>

- Shupe, M. D., Persson, P. O. G., Brooks, I. M., Tjernstrom, M., Sedlar, J., Mauritsen, T., et al. (2013). Cloud and boundary layer interactions over the Arctic sea ice in late summer. *Atmospheric Chemistry and Physics*, 13, 9379-9399. <https://doi.org/10.5194/acp-13-9379-2013>
- Soden, B. J., I. M. Held, R. Colman, K. M. Shell, J. T. Kiehl, and C. A. Shields (2008), Quantifying climate feedbacks using radiative kernels. *J. Climate*, **21**, 3504-3520, <https://doi.org/10.1175/2007JCLI2110.1>.
- Sohn, B.-J., J. Schmetz, R. Stuhlmann, and J.-Y. Lee (2006), Dry bias in satellite-derived clear-sky water vapor and its contribution to longwave cloud radiative forcing. *J. Climate*, **19**, 5570–5580, <https://doi.org/10.1175/JCLI3948.1>.
- Solomon, A., M. D. Shupe, P. O. G. Persson, and H. Morrison (2011), Moisture and dynamical interactions maintaining decoupled Arctic mixed phase stratocumulus in the presence of a humidity inversion, *Atmos. Chem. Phys.*, 11, 10,127–10,148, doi:10.5194/acp-11-10127-2011.
- Solomon, A., et al. (2014), The sensitivity of springtime Arctic mixed-phase stratocumulus clouds to surface-layer and cloud-top inversion layer moisture sources, *J. Atmos. Sci.*, 71, 574–595.
- Stramler, K., A. D. Del Genio, and W. B. Rossow (2011), Synoptically driven Arctic winter states. *J. Climate*, **24**, 1747-1762, <https://doi.org/10.1175/2010JCLI3817.1>.
- Tan, I., and Storelvmo, T. (2019). Evidence of strong contributions from mixed-phase clouds to Arctic climate change. *Geophysical Research Letters*, 46(5), 2894-2902. <https://doi.org/10.1029/2018GL081871>
- Tan, I. and D. Barahona (2022), The impacts of immersion ice nucleation parametrizations on Arctic mixed-phase stratiform cloud properties and the Arctic radiation budget in GEOS-5. *J. Climate*, **35**, 4049-4070. <http://doi.org/10.1175/JCLI-D-21-0368.1>.
- Tan, I., Sotiropoulou, G., Taylor, P.C., Zamora, L. and Wendisch, M. (2023). A Review of the Factors Influencing Arctic Mixed-Phase Clouds: Progress and Outlook. In *Clouds and Their Climatic Impacts* (eds S.C. Sullivan and C. Hoose). <https://doi.org/10.1002/9781119700357.ch5>.
- Taylor, P. C., Kato, S., Xu, K.-M., & Cai, M. (2015). Covariance between Arctic sea ice and clouds within atmospheric state regimes at the satellite footprint level. *Journal of Geophysical Research: Atmospheres*, 120(24), 12656–12678. <https://doi.org/10.1002/2015JD023520>
- Taylor, P. C., W. Maslowski, J. Perlwitz, and D. J. Wuebbles (2017). Arctic Changes and their Effects on Alaska and the Rest of the United States. In: *Climate Science Special Report: Fourth National Climate Assessment, Volume I* [Wuebbles, D. J., S. W. Fahey, K. A. Hibbard, D. J. Dokken, B. C. Steward, and T. K. Maycock (eds.)]. U.S. Global Climate Change Research Program, Washington, DC, USA, pp. 303-332, doi: 10.7930/J00863GK.

Taylor, P. C., R. C. Boeke, Y. Li, and D. W. J. Thompson (2019). Arctic cloud annual cycle biases in climate models, *Atmos. Chem. Phys.*, **19**, 8759–8782, <https://doi.org/10.5194/acp-19-8759-2019>.

Taylor P. C., Boeke R. C., Boisvert L. N, Feldl N., Henry M., Huang Y., Langen P. L., Liu W., Pithan F., Sejas S. A. and Tan I. (2022). Process Drivers, Inter-Model Spread, and the Path Forward: A Review of Amplified Arctic Warming. *Front. Earth Sci.* 9:758361. doi: 10.3389/feart.2021.758361

Taylor, P. C., and E. Monroe (2023), Isolating the surface type influence on Arctic low-clouds. *Journal of Geophysical Research: Atmospheres*, 128, e2022JD038098. <https://doi.org/10.1029/2022JD038098>

Tselioudis, G. and coauthors (2021), Evaluation of clouds, radiation, and precipitation in CMIP6 models using global weather state derived from ISCCP-H cloud property data. *J. Climate*, **34**, 7311–7324, <https://doi.org/10.1175/JCLI-D-21-0076.1>.

Van Weverberg, K., Boutle, I. A., Morcrette, C. J., and Newsom, R. K. (2016), Towards retrieving critical relative humidity from ground-based remote-sensing observations, *Q. J. Roy. Meteorol. Soc.*, 142, 2867–2881, <https://doi.org/10.1002/qj.2874>.

Vihma, T., Pirazzini, R., Fer, I., Renfrew, I. A., Sedlar, J., Tjernström, M., et al. (2014). Advances in understanding and parameterization of small-scale physical processes in the marine Arctic climate system: A review. *Atmospheric Chemistry and Physics*, 14, 9403–9450. <https://doi.org/10.5194/acp-14-9403-2014>

Voigt A, Albern N, Ceppi P, Grise K, Li Y, Medeiros B (2021), Clouds, radiation, and atmospheric circulation in the present-day climate and under climate change. *WIREs Clim Change*, Voigt A, Albern N, Ceppi P, Grise K, Li Y, Medeiros B. Clouds, radiation, and atmospheric circulation in the present-day climate and under climate change. *WIREs Clim Change*. 2021; 12:e694. <https://doi.org/10.1002/wcc.694> (e694), <https://doi.org/10.1002/wcc.694>.

Walters, D., Baran, A. J., Boutle, I., et al. (2019), The Met Office Unified Model Global Atmosphere 7.0/7.1 and JULES Global Land 7.0 configurations, *Geosci. Model Dev.*, 12, 1909–1963, <https://doi.org/10.5194/gmd-12-1909-2019>.

Wilson, D. R., Bushell, A. C., Kerr-Munslow, A. M., Price, J. D., and Morcrette, C. J. (2008a), PC2: A prognostic cloud fraction and condensation scheme. I: Scheme description, *Q. J. Roy. Meteorol. Soc.*, 134, 2093–2107, <https://doi.org/10.1002/qj.333>, 2008a.

Wilson, D. R., Bushell, A. C., Kerr-Munslow, A. M., Price, J. D., Morcrette, C. J., and Bodas-Salcedo, A. (2008b), PC2: A prognostic cloud fraction and condensation scheme. II: Climate model simulations, *Q. J. Roy. Meteorol. Soc.*, 134, 2109–2125, <https://doi.org/10.1002/qj.332>.

Yeo, H., M.-H. Kim, S.-W. Son, J.-H. Jeong, J.-H. Yoon, B.-M. Kim, S.-W. Kim (2022), Arctic cloud properties and associated radiative effects in the three newer reanalysis datasets (ERA5, MERRA-2, JRA-55): Discrepancies and possible causes, *Atmos. Res.*, **270**, <https://doi.org/10.1016/j.atmosres.2022.106080>.

Yu, Y., Taylor, P. C., & Cai, M. (2019). Seasonal variations of Arctic low-level clouds and its linkage to sea ice seasonal variations. *Journal of Geophysical Research: Atmospheres*, 124(2), 12206-12226. <https://doi.org/10.1029/2019JD031014>

Zelinka, M. D., Myers, T. A., McCoy, D. T., Po-Chedley, S., Caldwell, P. M., Ceppi, P., et al. (2020). Causes of higher climate sensitivity in CMIP6 models. *Geophysical Research Letters*, 47, e2019GL085782. <https://doi.org/10.1029/2019GL085782>.

Zelinka, M.D., and coauthors (2023), Detailing cloud property feedbacks with a regime-based decomposition. *Clim Dyn.*, **60**, 2983–3003, <https://doi.org/10.1007/s00382-022-06488-7>.